SIMULATION OF EARTH-TO-AIR HEAT EXCHANGER SYSTEMS

Min Zhong Zhao

A Thesis

in

The Department

of

Building, Civil and Environmental Engineering

Presented in Partial Fulfillment of the Requirements
For the Degree of Master of Applied Science at
Concordia University
Montreal, Quebec, Canada

April 2004

ABSTRACT

SIMULATION OF EARTH-TO-AIR HEAT EXCHANGER SYSTEMS

Min Zhong Zhao

Solar energy accumulated in the soil may be utilized with earth-to-air heat exchangers (ETAHEs), which have a single tube or a group of tubes buried into the ground. When the ventilation air is drawn through the tube(s), the air is heated in winter and cooled in summer due to the temperature difference between the air and the ground. By taking advantage of this free energy, we can reduce the energy consumption required for space conditioning.

The use of such a system requires a complex dimensioning process, which involves optimization of numerous parameters such as the airflow rate, tube length, depth, and diameter; in the meantime, some potentially adverse aspects of the system such as condensation have to be considered. Various algorithms to calculate the performance of a single or multiple earth-to-air heat exchangers have been proposed. However, these algorithms are either too complicated to be utilized by a design engineer or too simple to consider latent heat transfer and transient effects.

In this thesis, first a transient control volume model is presented to investigate the transient soil heat rejection around an ETAHE. Then, a 1-D steady-state model is developed by combining a control volume model with an analytical solution for prediction of ETAHE outlet temperature, relative humidity and condensation (if any). The model is validated against two sets of published experimental data. By trying various combinations of different parameters, one may find an optimal dimension for an ETAHE system. Application of this technique in Montreal climate is also analyzed.

ACKNOWLEDGMENTS

TABLE OF CONTENTS

LIST OF FIGURES AND TABLES

x

NOMENCLATURE

English Letters

A	*area [m^2]*
A_p	*perimeter [m]*
A_s	*amplitude of surface temperature variation [°C]*
C	*thermal capacity [J/K]*
c	*specific heat capacity [J/kg K]*
D	*tube diameter [m]*
$D_{u,vap}$	*isothermal diffusivity of moisture in vapor form [m^2/s]*
D_T	*thermal moisture diffusivity [m^2/s K]*
D_u	*isothermal moisture diffusivity [m^2/s]*
D_v	*vapor diffusivity [m^2/s]*
f_a	*heat transfer enhancement factor*
h	*moisture content [kg of moisture / kg of dry soil]*
h_c	*convection coefficient [W/m^2 K]*
h_m	*mass transfer coefficient [m/s]*
H_{fg}	*latent heat of condensation [kJ/kg]*
k	*conductivity [W/m K]*
L	*tube length [m]*
l_g	*moisture heat of vaporization [kJ/kg]*
m	*mass flow rate [kg/s]*
N	*control volume number*

Nu	Nusselt number
P	standard atmospheric pressure [Pa]
P_v	partial vapor pressure [Pa]
P_s	saturated vapor pressure [Pa]
Pr	Prandtl number
Q	heat flux [W/m²]
r	polar co-ordinate, radial distance from the tube axis [m]
R	thermal resistance [°C/W]
Re	Reynolds number
RH	relative humidity
T	temperature [°C]
t_0	duration of year [s]
t	time [s]
T_a	air temperature inside the tube [°C]
T_s	temperature of tube surface [°C]
T_m	annual mean value of ambient air temperature [°C]
T_{max}	annual maximum value of ambient air temperature [°C]
T_o	ambient air temperature [°C]
U	heat transfer coefficient between air and wall of the tube [W/ m²K]
U_L	heat transfer coefficient per meter of wall of tube [W/ mK]
V	air velocity [m/s]
W	humidity ratio [kg water/kg dry air]
W	power [W]

w	moisture content of soil [%]
x	distance [m]
y	polar coordinate, axial distance from the tube inlet [m]
z	depth of the tube center under surface [m]

Greek symbols

α	thermal diffusivity [m^2/s]
η	efficiency
ρ	density [kg/m^3]
v	kinematic viscosity [m^2/s]
ω	angular frequency [s^{-1}]
ξ	dimensionless parameter for thermal depth of tube

Subscript

a	air
i	number of node
j	number of node
o	outdoor or inlet
s	soil
so	undisturbed soil

CHAPTER 1

INTRODUCTION

1.1 Background

Saving energy is one of the most important global challenges in our days. The energy crisis of the mid-1970s dealt a harsh blow to developed countries including Canada. The most beneficial outcome of the crisis is that it stimulated interest in the diversification of energy sources and renewable energy.

Meanwhile, environmental concerns push this trend much further. In order to reduce greenhouse gas (GHG) emissions, which are considered to be culprit of global warming and sources of pollution, the Kyoto protocol set specific targets for reduction of CO_2 emissions. Under this agreement, Canada is committed to cut GHG emissions by 6% below 1990 levels by 2012. This regulation has encouraged two important initiatives. First of all efforts are focused on producing electricity with higher efficiency. Old power plants are more rapidly phased out and replaced by new, more efficient plants. Secondly, the attention was drawn on energy use. More efficient use of energy not only reduces the consumption of electricity, but also lowers the consumption of primary energy sources.

Buildings, whether residential or commercial, mainly use energy to obtain comfort for their inhabitants. This comfort is visual, ergonomic, but mainly thermal. In order to reduce energy consumption of buildings, several passive techniques are nowadays introduced in HVAC installations. In many cases solar energy is directly or indirectly used to supply heat or electrical energy. Sometimes solar gains inside the building are

1

avoided to reduce cooling needs or the size of the air-conditioning unit. Other techniques are based on recovering heat or even 'cold'. In most cases several passive measures are combined.

Earth as a heat source and heat sink is a well-studied topic. Using the earth as a component of the energy system, or "earth-tempering," can be accomplished through three primary methods: direct, indirect, and isolated. In the direct system, the building envelope is in contact with the earth, and conduction through the building elements (primarily walls and floor) regulates the interior temperature. In the indirect system, the building interior is conditioned by air brought through the earth, such as in earth-to-air heat exchangers (ETAHEs). The isolated system uses earth temperatures to increase the efficiency of a heat pump by moderating temperatures at the condensing coil. A geothermal heat pump is an example of an isolated system. This thesis will focus on indirect systems.

Indirect systems, i.e. earth-to-air heat exchangers systems, sometimes called ground tubes, or ground-coupled air heat exchangers are an interesting and promising technology. Tubes are placed in the ground, through which air is drawn (see Figure 1.1). Because of the high thermal inertia of the soil, the air temperature fluctuations at the ground surface exposed to the exterior climate are damped deeper in the ground. Further a time lag occurs between the temperature fluctuations in the ground and at the surface. Therefore at a sufficient depth the ground temperature is lower than the outside air temperature in summer and higher in winter. When fresh ventilation air is drawn through the earth-to-air heat exchangers the air is thus cooled in summer and heated in winter. In combination with other passive systems and good thermal design of the building, the

earth-to-air heat exchanger can be used to preheat air in winter and avoid air-conditioning units in buildings in summer, which results in a major reduction in electricity consumption of a building.
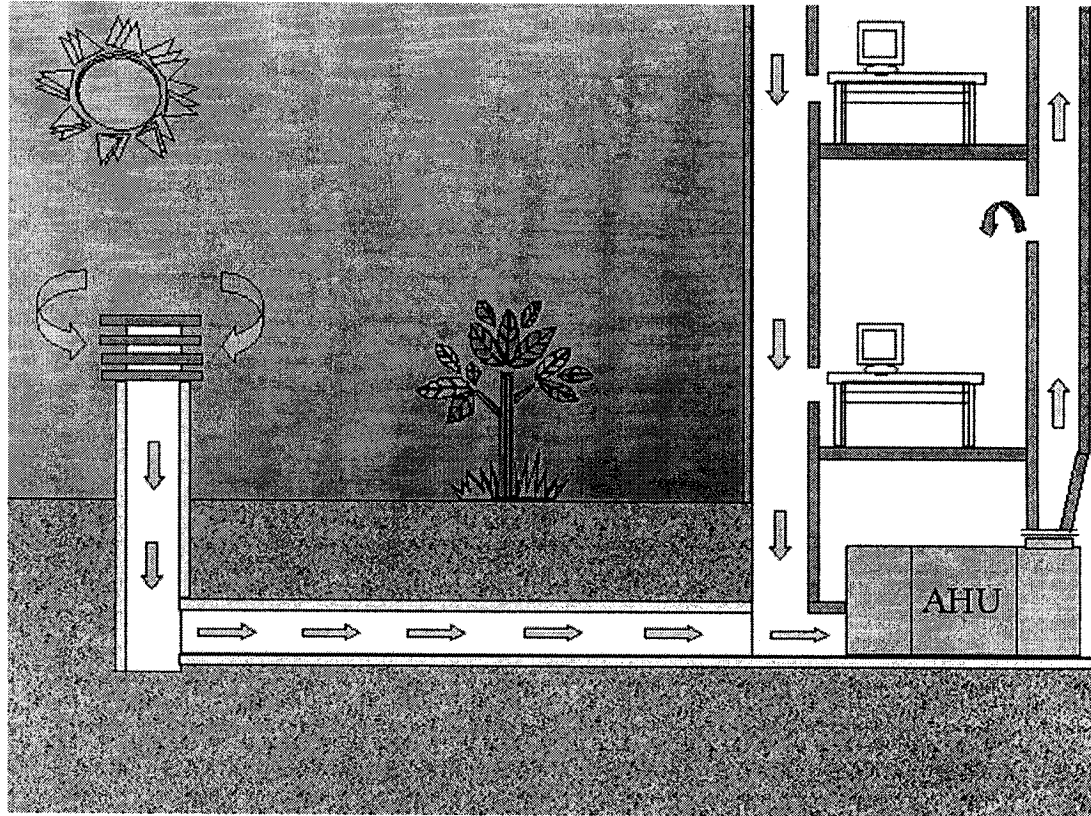
Fig. 1.1 Schematic diagram of an earth-to-air heat exchanger (ETAHE) and a building

1.2 Motivation

In the literature, numerous models, either 1-D or multi-dimensional ones, have been developed to predict the performance or to optimize the design of earth-to-air heat exchanger systems. Although theoretically they accommodate more details of this

3

physical behaviour, 3-D models, are usually quite complex and do not consider simultaneously transient effects due to change of the soil temperature and condensation. 1-D models, on the other hand, may characterize the behaviour of the earth-air heat exchangers accurately enough as Tzaferis et al [1992] reported. However, few of them can predict transient effects and latent heat transfer, which may lead to condensation in the ETAHE and affect the indoor air quality (IAQ). Hence, in order to take into account both sensible and latent heat transfer, there is a need to develop a practical 1-D model so that the design engineer may optimize the system both easily and accurately.

1.3 Objectives

The main objectives of the thesis are as follows:

1. To perform an extensive literature review to identify the research and development status of this technique and current guidelines for designing earth-to-air heat exchanger systems.

2. To develop a transient thermal network model for finding the transient temperature profile around an earth tube in order to determine the optimal depth of the earth-to-air heat exchanger systems and the change of temperature of the soil due to prolonged usage.

3. To develop a new methodology for simulation of the earth tube system taking into account both heat transfer and condensation.

4. To apply this technology to Montreal climate.

1.4 Organization of the thesis

Chapter 2 describes the previous and present applications of this specific technique, and also presents a literature review on a variety of models to show the present research progress and its limits.

Chapter 3 studies the ground heat and mass transfer mechanisms. By simplifying them, a numerical simulation of heat conduction around a tube is performed to find the optimal depth of the earth tube system.

Chapter 4 studies a numerical simulation model of a single open-loop earth-tube in both heating and cooling cases. The temperatures and relative humidities of every node along the tube are found by using a control volume method. Comparisons of the numerical results with experimental results are then made. A sensitivity analysis further verifies some design guidelines. Finally, simulations for Montreal climate are presented in order to evaluate the application possibility of this specific technology.

Chapter 5 gives the conclusions and recommendation of future work.

CHAPTER 2

LITERATURE REVIEW

2.1 Introduction

The use of the earth as a heat source or as a heat sink, which, in combination with buried tubes, can serve as a direct heat exchanger, is an old concept that has existed in Persian architecture for centuries [Trombe et al, 1994]. In literature, the system is usually called Earth-to-air heat exchanger(s) (ETAHE or EAHXs) [Tzferis et al, 1992; Mihalakakou et al, 1994 and 1996b; Santamouris et al, 1995a; Bojic et al, 1999; Nara et al, 2000; Gieseler et al, 2002; De Paepe et al, 2003; Pfafferott, 2003]. But it is also called:

1. Buried pipe system [Hollmuller et al 2003b; Mihalakakou et al, 1995, 1996a and 2003]

2. Hypocaust [Hollmuller et al, 2003a]

4. Air-to-earth heat exchanger (ATE) [Trombe et al, 1994; Bojic et al, 1997]

6. Underground air tunnel [Goswami et al, 1985 and 1990]

7. Earth-tube heat exchanger [Gustafsson, 1993; Bourret et al, 1994; Lemay et al, 1994 and 1995; Dhia, 1995; Levit et al, 1989]

8. Air-soil heat exchanger [Hollmuller, 2003a]

9. Earth air tunnel [Bansal et al, 1986; Arzano et al, 1994; Kaushik et al, 1994; Kumar et al, 2003]

Throughout the thesis, the term of Earth-to-air heat exchanger (ETAHE) is employed.

2.2 ETAHE applications

All over the world, this technique is implemented in a variety of buildings (see Table 2.1.). But most of them are in European countries [Hokkaner, 1994; Mihalakakou et al,

6

1996a; Wagner et al, 2000 and De Paepe et al, 2001]. Many ETAHE systems have been applied to greenhouses [Mavroyanopoulos et al, 1986; Boulard et al, 1989; Levit et al, 1989; Santamouris et al, 1994 and 1995b; Sutar et al, 1996; Gauthier et al, 1997; Tiwari et al, 1998 and Nara et al, 2000], and livestock houses [Lemay et al, 1994 and 1995; Shingari, 1995; Dhia, 1995]. For livestock housing latent and sensible heat production is very high due to the high concentration of animals in the building. To maintain animal health, and consequently to improve the efficiency of animal production, ventilation requirements are such important that it is necessary to keep a high value of air flow rate. Correia et al [2001] studied a livestock building with ETAHEs and a solar chimney and made a conclusion that the thermal environment inside the building stays about 91% of the time within the thermoneutral zone. High temperature during the summer season and low temperature in winter are also adverse to greenhouse crops. The ETAHE, which is one of the passive solar systems, has been installed in greenhouses as a heating and cooling system over last thirty years. Santamouris et al [1995b] investigated into 18 greenhouses (See Table 2.2.) with installation of ETAHE systems all over the world. They concluded that these applications show good performance and effectiveness for both heating and cooling. In addition to reduce loads, Nara et al [2000] furthered a step to use ETAHE systems to collect condensation to compensate the water needs of a greenhouse as well as to condition the greenhouse.

Recently, more and more ETAHE systems found them applied not only in residential buildings [Bowman et al, 1987; Arzano et al, 1994] but also commercial and institutional buildings. In literature reports applications included a hospital complex [Sodha et al, 1985], university buildings [Meliß et al, 2000; Athienitis et al., 2002], a cinema hall

[Singh et al, 1996], etc. All of these reports demonstrate that the ETAHE technique has a promising contribution to reducing cooling and heating loads.

In Canada, there are only two ETAHE applications identified in various publications. One is a greenhouse [Santamouris et al, 1995b], while the other is a growing-finishing swine building [Lemay, 1994 and 1995]. They are all in Quebec. Right now, the Cité du Cirque with ETAHE system in Montreal is under construction. This project opens a new era that this technology begins to be employed on a wider scale in Canada.

2.3 Review of models

The various models are summarized and detailed in Table 2.3.

2.3.1 Multi-dimensional models

To predict the performance of the ETAHE system, Mihalakakou et al [1994], Bojic et al. [1997], Gauthier et al [1997] and Hollmuller et al [2003b] have developed some complete and dynamic models for ETAHEs. These models differ in the way the geometry is described (2D, 3D, polar coordinates) and in the way the effects of moisture transport in the ground and in the air are accounted for. However, these calculation methods are quite complex and their solutions are usually obtained by using commercial software such as TRNSYS, ANSYS, SMILE and FLUENT etc. Therefore, the applicability for design is limited to people who are able to use the calculation codes or software. They are mainly used to show that the ETAHE is a promising and effective technology.

The heat transfer model is based on the following assumptions:

1. Conduction heat transfer is transient and fully three dimensional in the soil.

2. The thermo physical properties of the soil and other materials are constant.

3. Heat transfer by moisture gradients in the soil is neglected.

4. Heat transfer in the tube is dominated by convection. It is coupled with the temperature field of the surrounding soil by the boundary conditions at the tube surface.

2.3.2 One-dimensional models

In the literature several one-dimensional calculation models for ETAHEs are found. Tzaferis et al. [1992] studied eight models. Six of the models use a steady-state one-dimensional description of the tube. The algorithms are classified in two groups:

1. The algorithms that first calculate the convective heat transfer from the circulating air to the tube and then calculate the conductive heat transfer from the tube to the ground inside the ground mass. The necessary input data are:

- the geometrical characteristics of the system

- the thermal characteristics of the ground

- the thermal characteristics of the air

- the undisturbed ground temperature during the operation of the system.

2. Those algorithms that only calculate the convective heat transfer from the circulating air to the tube. In this case the necessary input data are:

- the geometrical characteristics of the system

- the thermal characteristics of the air

- the temperature of the tube surface

A relation between inlet and outlet temperatures of the tube is derived. For all of these models no influence of thermal capacity of the earth can be taken into account. Secondly the influence of different tubes on each other cannot be studied. In one algorithm the

9

Table 2.1 Earth-to-air heat exchanger applications around the world

Location & function	Reporter	Tube					Depth (m)	Air	
		Material	Length (m)	Diameter (mm)	No.	Layout		Velocity (m/s)	Flow rate(m³/s)
Germany Office	Pfafferott, 2003	PE	67-107	200 &300	26		2-4	2.2	10300
Germany Office	Pfafferott, 2003	PE	95	250	7		2	5.6	7000
Germany Office	Pfafferott, 2003	PE	Each 90	350	2		2.3	1.6	1100
Germany, House	Benkert, 1998		42	125	1		0.7-1.8		140
Yugoslavia	Bojic, 1999	PVC & Steel	50	125	1		1.5		
Germany, Office	Wagner, 2000	Concrete	32	500	4	Parallel (P)	1.5	1.2	3400
Canada, Swine House	Lemay, 1994	PVC	61	300	11	(3m)	3		1258 l/s
Switzerland, Greenhouse	Hollmuller, 1999	PVC	11	160	24	P (0.33m)	0.8		
Switzerland, Office	Hollmuller, 1999		23	250	43	P (1.16m)	0.75basement 6 ground		6000-18000
Greece, Experiment	Mihalakakou, 1994	PVC	14.8	150	1		1.1		
Iraq, Poultry	Dhia, 1995	Steel	30	300(4)	1	U-shape	2.5		1200
India, Poultry	Shingari, 1995	PVC	13	200	3		1.7	4.5	

Table 2.2 Earth-to-air heat exchanger applications in greenhouses (Santamouris et al, 1995b)

Location	Surface (m²)	Cover material	Cultivation	Storage medium	Installed
Adana, TU	835	P.E.	--	Plastic (50 cm deep)	1984
Montreal, CA	100	Glass	Plants	Plastic (45 and 65 cm deep)	1986
Catania, IT	200	P.E.	--	Concrete (40 cm deep)	1989
Avignon, FR	176	Polycarbon	Vegetables	Concrete (0.4 and 0.8 m deep)	1985
Quebec, CA	72	Fiberglass	Plants	Plastic (30 and 60 cm deep)	1985
Jange, FR	1470	--	--	Rough cast (45 cm deep)	1985
Bukhara, USSR	--	--	Plants	Plastic (40 cm deep)	1986
Nice, FR	3000	Glass	Eggplant	Plastic (80 cm deep)	1979
Rome, IT	1000	Glass	--	Concrete	1985
Iver, UK	1000	Glass	--	Concrete	1985
Yokohama, J	1736	Glass	Tomatoes	Plastic (0.5 and 0.9 cm deep)	1984
Athens, GR	150	P.E.	--	Aluminum (2m deep)	1981
Valencienne, FR	58	Double P.E.	Plants	Plastic (2 and 2.1m deep)	1980
Agrinio, GR	1000	Fiberglass	Roses	Plastic (1.5m deep)	1986
Athers, GR	1000	Glass	Flowers	Plastic (1.5m deep)	1988
Volos, GR	2500	Polycarbon	--	Plastic (1.2 and 1.8m deep)	1991
Kumano, J	46	Plastic	--	Plastic (50 cm deep)	1988
Saintes, FR	297	P.E.	--	Plastic (1.2m deep)	--

Table 2.3 Earth-to-air heat exchanger (ETAHE) multi-dimensional models
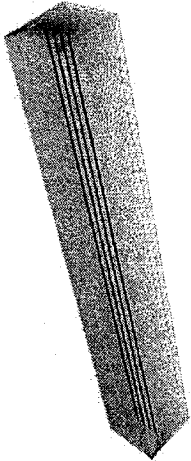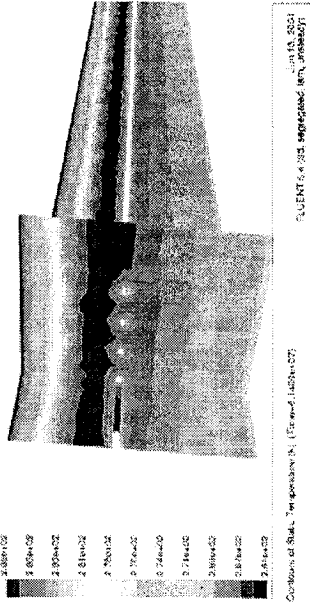
Model Proposer & Year	Summary	Important diagrams, equations and results	Tools for Solutions	Remarks
Mihalakakou, 1994	2-D Transient Implicit Cylindrical coordinate CVM	$$\rho c_p \frac{\partial T_s}{\partial t} = \frac{1}{r}\frac{\partial}{\partial r}\left(k_s r \frac{\partial T_s}{\partial r}\right) + \frac{\partial}{\partial y}\left(k \frac{\partial T_s}{\partial y}\right) - l_g \rho_m \frac{1}{r}\frac{\partial}{\partial r}\left(D_{u,vap} r \frac{\partial h}{\partial r}\right) - l_g \rho_m \frac{1}{r}\frac{\partial}{\partial y}\left(D_{u,vap}\frac{\partial h}{\partial y}\right)$$ $$\frac{\partial h}{\partial t} = \frac{1}{r}\frac{\partial}{\partial r}\left(D_T r \frac{\partial T_s}{\partial r}\right) + \frac{\partial}{\partial y}\left(D_T \frac{\partial T_s}{\partial y}\right) - \frac{1}{r}\frac{\partial}{\partial r}\left(D_u r \frac{\partial h}{\partial r}\right) - \frac{\partial}{\partial y}\left(D_u \frac{\partial h}{\partial y}\right)$$	TRNSYS	Round single tube only Condensation predicted
De Paepe, 2002	Transient 3-D FVM Implicit	A typical calculation grid generated by Gambit: A cut through the calculation domain: 	FLUENT 3D and its UDF	No condensation predicted Finite tetrahedral volumes
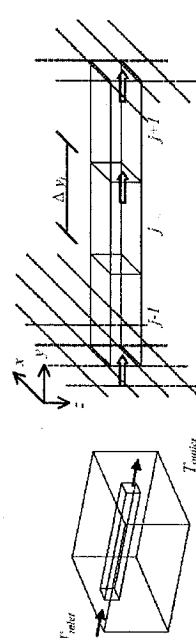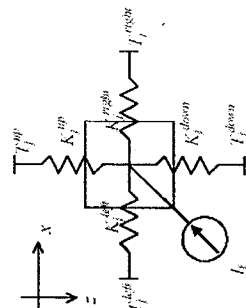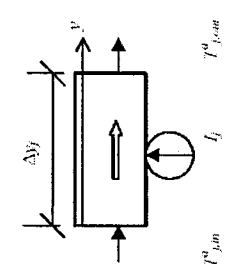
12

Table 2.3 (*Continued*)

Model Proposer & Year	Summary	Important diagrams, equations and results	Tools for Solutions	Remarks
Fredrik, 2000	Cartesian coordinate Transient	A schematic overview of the calculation region (left) and the air-channel (right). The region is divided into a number of computational cells. . The thermal conductances and latent heat generation Ij connected to calculation cell j in ETAHE (left). The airflow through an ETAHE segment j (right).	Matlab	Rectangular tube, no condensation predicted
Chen et al., 1990	3-D Transient FDM	$$T_a^{x+1} = \frac{4U}{\rho_a c_a DV} T_s\, dx + T_a^x \left(1 - \frac{4U}{\rho_a c_a DV}\, dx \right)$$		

Table 2.3 (*Continued*)
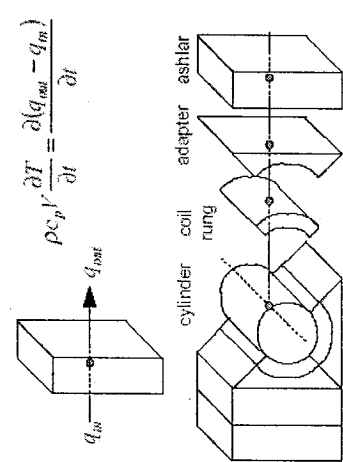
Model Proposer & Year	Summary	Important diagrams, equations and results	Tools for Solutions	Remarks
Wagner, 2002	Cylindrical and Cartesian coordinates	$$\rho c_p V \frac{\partial T}{\partial t} = \frac{\partial (q_{out} - q_{in})}{\partial t}$$ Different control volumes for the ground and the tubes. The material properties can be set individually. Heat flux is allowed in only radical direction	SMILE	No condensation predicted

14

Table 2.4 Earth-to-air heat exchanger (ETAHE) 1-D models

Model Proposer & Year	Summary	Important diagrams, equations and results	Tools for Solutions	Remarks
Athienitis, 2001	Steady-state Explicit	$T_a(x) = T_s - (T_s - T_o)\exp(-x/a)$ where $a = \dfrac{\dot{m}C_a}{A_p h_c}$	ODE MathCAD	Exact Solution; Heat diffusion in ground ignored; No condensation predicted
Benkert, 1998	Steady-state Explicit FDM	$T_s = \dfrac{UT_{s0} + T_a}{U+1}$ where $U = 2\pi \dfrac{k_s}{U_L} \cdot \dfrac{1}{\ln\left(\dfrac{z}{R} + \sqrt{\left(\dfrac{z}{R}\right)^2}\; -1\right)}$ Both undisturbed earth temperature and ambient air temperature are assumed as a sinusoidal.	VB	GAEA; No condensation predicted
Schiller, 1982	1-D Transient Explicit	$T_a^{x+1} = T_a^x - \dfrac{Q_x}{\dot{m}c_a}$ Convective heat transfer in the tube and conductive in the ground are treated simultaneously		No condensation predicted; Unrealistic prediction
Santamouris, 1986	1-D FDM	$T_a = (T_o - T_s)\exp(-Sa)[1 + (BiSa)^{0.5}]$ $\times \displaystyle\int_0^{Fo} \exp(-BiFo)I_1(2[BiSaFo]^{0.5})Fo^{0.5}\,dFo] + T_s$ Bi, Sa and Fo are dimensionless parameters		No condensation predicted

15

Table 2.4 (*Continued*)

Model Proposer & Year	Summary	Important diagrams, equations and results	Tools for Solutions	Remarks
Levit, 1989	1-D Steady-state Explicit FDM	$$T_a^{x+1} = T_a^x \frac{\dot{m}c_a - UAdx}{\dot{m}c_a} + \frac{UAdx}{\dot{m}c_a} T_s(x,D)$$ with $A = 2\pi D$, U is the overall heat transfer coefficient, $T_s(x,D)$ is the ground temperature at length x at a distance D from the tube and dx the length of the elementary part of the tube		No condensation predicted
Sodha et al, 1984	1-D FDM	$$T_a = T_s \left((T_o/T_s - 1)\exp(-\beta n) + 1 + F(n, \frac{2\pi R_i LU}{\dot{m}c_a}) \right)$$		No condensation predicted
Benkert, 1998	1-D Steady-state Explicit FDM	$$T_a^{x+1} = \frac{(1 - U/2)T_a^x + UT_s}{(1 + U/2)}$$ where $U = (2\pi R dx U_w)/\dot{m}c_a$		GAEA; Condensation predicted

ground is divided into co-axial cylindrical elements. The thermal resistance of the ground is considered to be time-dependent. The tube is divided in segments. In each segment the exit temperature is determined. In another algorithm the steady-state heat balance is solved between a point in the ground and the tube. It is concluded that the different models give comparable results. This is mainly caused by the fact that the models offer different solution methods and dicretisations of the same equations. The compliance with measurements done by Tzaferis et al (1992) is quite good. This shows that a steady-state one-dimensional model may characterize the behaviour of the ETAHEs. This approach will be followed in this thesis.

2.4 Design guidelines

2.4.1 Important design parameters

2.4.1.1 Tube depth

Obviously, tubes should be placed as deep as possible. The ground temperature is defined by the external climate and by the soil composition, its thermal properties and water content. The ground temperature fluctuates in time, but the amplitude of the fluctuation diminishes with increasing depth of the tubes, and deeper in the ground the temperature converges to a practically constant value throughout the year.

It was studied that tubes should be buried at least 1.5 meters below grade, but only rarely is burying them more than 3.5 meters justifiable [EREC, 2002]. The required tube depth is also strongly influenced by surface conditions since exposed sites without trees or ground cover have much higher subsurface ground temperatures in summer. Although the simplicity and reasonable cost are tempting, ground temperatures at 1m are usually too high for useful cooling or too low for preheating in majority of Canadian cities.

17

Increased tube length cannot compensate for ground temperatures [Abrams, 1986].

Several types of powered trenching devices are available nowadays, but most can dig only to a depth of 2m or less [EREC, 2002]. When digging trenches much deeper, cave-ins are an extreme hazard, and appropriate precautions should be taken.

2.4.1.2 Tube length, tube diameter and air flow rate

The total surface area of the ETAHE, a key factor in overall cooling capacity, may be increased by two means: increasing the diameter or increasing the tube length. However, increased diameter reduces air speed and heat transfer, and greater length increases the pressure drop through the tube and increases fan energy. Usually, the correct design solution is a set of parallel tubes each with the proper diameter for best overall performance [EREC, 2002].

Optimum tube diameter varies widely with tube length, tube costs, flow velocity, and flow volumes. Diameters between 150mm and 450mm appear to be most appropriate [IEA, 1999]. Long tubes are not needed. The air temperature in the tube reaches the ground temperature quickly. Thermal performance and pressure drop both grow with length. Smaller tube diameters give better thermal performance, but also larger pressure drop [EREC, 2002].

A diameter should be selected that it can balance the thermal and economic factors for the best performance at the lowest cost. The optimum is determined by the actual cost of the tube and the excavation. Excavation costs in particular vary greatly from one location and soil type to another.

For a given tube diameter, an increase in airflow rate will increase the film coefficient

18

and increase both total heat transfer and outlet temperature. This implies that high airflow rates are desirable for closed systems. However, for open systems, the airflow rate must be selected by consideration of both the required outlet temperature and total cooling or heating capacity.

2.4.1.3 Tube material

The main considerations in selecting tube material are cost, strength, corrosion resistance, and durability. Tubes made of concrete, metal, plastic, and other materials have been used. Simulations indicate tube material has little influence on performance. Increasing the conductivity of the tube to a value corresponding to that of aluminum increased total heat transfer by less than 10% [Abrams, 1986]. Bojic et al [1999] studied two earth tubes: one PVC tube, and the other steel tube. They have the same dimension and parallel with each other. Results showed that steel tube heat contribution account for no more than 54% of heat output from the two tubes. PVC or polypropylene tubes perform almost as well as metal tubes [EREC, 2002]: they are easier to install, and are more corrosion resistant.

2.4.2 Tube arrangement

2.4.2.1 Open-loop system *vs.* closed-loop system

An ETAHE uses either an open loop or closed loop configuration. In an open-loop system, outdoors air is drawn into the tubes and delivered to air handing units (AHUs) or directly to the inside of the building. This system provides ventilation while hopefully cooling or heating the building's interior. In a closed-loop system interior air circulates

through the ETAHEs. Using a closed loop results in the best efficiency and reduces problems with humidity condensing inside the tubes [Abrams, 1986].

2.4.2.2 One-tube system *vs.* parallel tubes system

To meet given air conditioning requirements of a given building space, air through one tube may not be adequate or the size of the required tube may be too large. In such a case one may use more than one tube, buried in the ground, parallel to each other, to meet the given load requirements, taking into account the influence of the tubes on each other. To prevent interference between the individual tubes, the distance between them should be at least 1 m [De Paepe et al, 2003].

More tubes in parallel both lower pressure drop and raise thermal performance [De Paepe et al, 2003]. Studies showed that multiple small tubes optimize performance [EREC, 2002]. However, other research [IEA, 1999] indicated that parallel 300mm tubes typically offer the highest energy and cost efficiencies.

2.4.3 Efficiency and COP

2.4.3.1 ETAHE efficiency

Calculating benefits from the use of ETAHEs is difficult due to fluctuating soil temperatures and conductivity. ETAHE efficiency may give a clue in evaluating their performance. It is defined by:

$$\eta = \frac{T_o - T_a(L)}{T_o - T_s} \tag{3.1}$$

where T_o is the inlet air temperature and $T_a(L)$ is the outlet air temperature after the

ETAHE with a length of L. T_s is the undisturbed ground temperature at the depth of the buried tubes. It was studied [Gieseler, 2002] that for small units the efficiency is usually not much higher than 0.5.

2.4.3.2 COP

The system COP is based on the amount of cooling or heating produced by the ETAHE and the amount of power required moving the air through the ETAHE. That is:

$$COP = \frac{\sum Q}{W} \tag{3.2}$$

As the system is operated in summer, the soil temperature around the tube increases. When the system is shut off, heat is transferred within the soil, which reduces the soil temperature. During the shutoff period in summer, the soil moisture also diffuses back, thereby regenerating the soil for the next start-up period. However, as the system is operated day after day, the soil temperature for each day is higher than that during the previous day. This affects the outlet air temperature and the system COP. Goswami et al [1990] reported that the system COP decreases as the system is operated. However, the COP value is quite high, even after intermittent operation for 90 days (Figure 2.1). This shows the usefulness of this technique for passive cooling.

COP is such an important parameter that it can be integrated into system control strategies. When the COP of the system is reduced down to a specified value, the system should be shut off and the conventional air conditioner provides the entire load.
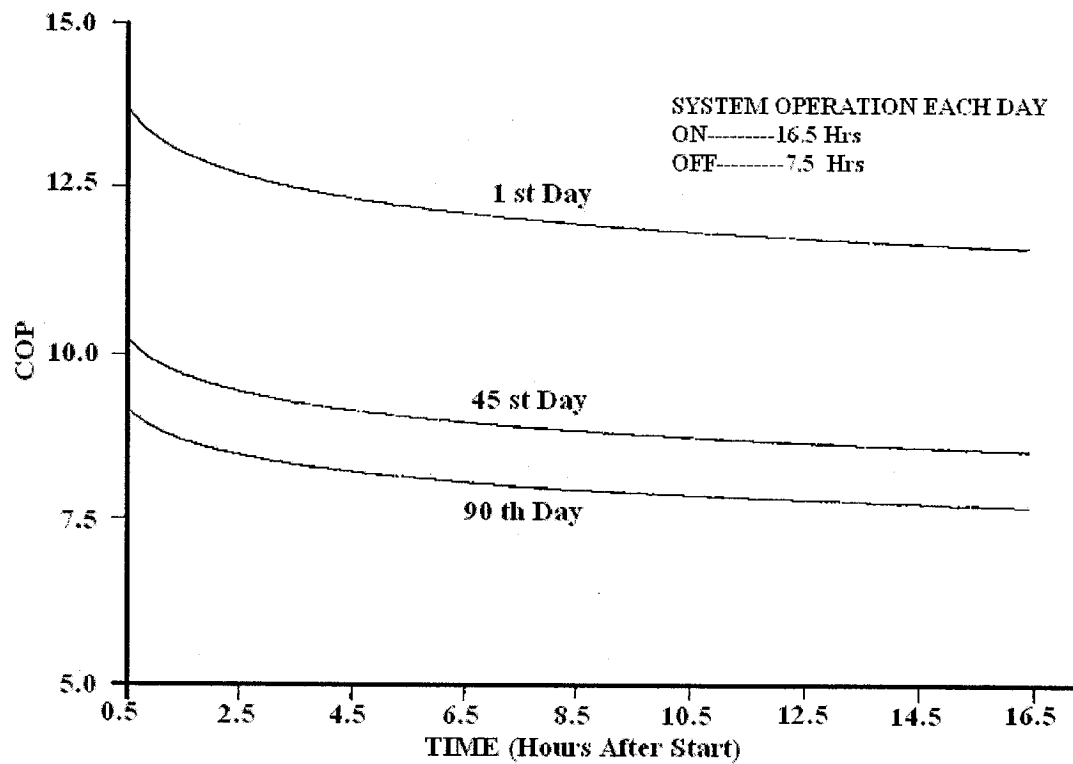
Fig. 2.1 COP of an ETAHE system for long-term operation (Goswami et al, 1990)

2.4.4 Controls

In operation, the control strategy plays a decisive role for the actually usable energy supply by the ETAHE. A temperature control is important to prevent unwanted heating in summer and cooling in winter. Of course, a better utilization of energy supply is achieved by a close loop control but its programming is difficult because of long dead time in ETAHE. An open loop control runs robustly but usually its programming should be adjusted after the first year of operation, when the temperature behaviour is known [Pfafferott, 2003].

In order to maximize the control of such a system it is necessary to provide an automatic control algorithm. This algorithm must compare the indoor temperature with

the temperature at the air outlet and, when the former is lower than the latter, the fan must be stopped. Obviously, if the system is to be linked with conventional air conditioning, the automatic control has to be more sophisticated.

2.5 Potential problems

2.5.1 Moisture accumulation and IAQ problem

The possibility of the forming of water by condensation inside the tubes has been well studied [Abrams, 1986]. Condensation will occur if the temperatures of the inside tube walls is lower than the dew point temperature of the air, which depends on the air temperature and on the humidity of the air. Condensation has been observed in some systems [Goswami et al, 1990], but only with very low airflow and high ambient dew point temperature. Reports of water flowing continuously from systems in the operation are probably attributable to groundwater leakage into the tubes [Labs, 1989].

Even if some moisture can be removed from the ambient air, it is even more difficult to dehumidify to normal interior comfort conditions. In cooling warm, humid air, an ETAHE system will always increase the relative humidity of the air. As air is cooled, its capacity to hold water is reduced. When cooled without moisture removal, air initially at 30°C and 60% RH will reach 70% RH at 28°C, 83% RH at 25°C and 98% RH at 21°C [Abrams, 1986]. Note that comfort for the human body is determined by relative humidity, not absolute moisture content. The discharge of humid air, even though it is cooler, into the interior of a building can cause discomfort, as well as mildew. Since the system may not be able to remove moisture from the air, it may have to be used in combination with a regular air conditioner or a desiccant.

23

Water in the tubes or corresponding structures can be a source for the growth of mould or mildew. This can cause a reduction in the indoor air quality, as spores can be responsible for respiratory problems or allergic reactions in humans. Mould and mildew grow on most surfaces if the relative humidity at the surface is above a critical value and the surface temperature is above 4°C [EREC, 2002]. The International Energy Annex 14 [IEA, 1999] established a surface humidity criterion for design purposes: the monthly average relative humidity at the surface should remain below 80%. So, if the monthly average humidity is above 80%, risk for moulds growing is imminent.

Good construction and drainage could eliminate condensation and groundwater. To avoid water standing in the tubes, the tubes are tilted 1° [Santamouris et al, 1996]. In a service pit at the lowest point of the tubes the water can be captured and pumped. The extraction pump is designed to take out the maximum calculated water flow rate. The slope will prevent the accumulation of large amounts of water, but cannot remove small puddles or moisture that adheres to the tube walls. Corrugated or convoluted tubes are particular problems [Abrams, 1986]. To ensure that no groundwater enters the tubes, PE-tubes may be used instead of concrete tubes since PE-tubes are fully watertight. To avoid water entering through bends and connections, these will be prefabricated and the whole tube systems will be connected above ground, after which the complete system will then be put into the ground [IEA, 1999].

2.5.2 Insects and rodents

Insects and rodents may enter the tubes of an open-loop system. A sturdy grille and insect screen should be installed at the tube inlet to deter potential intruders.

2.5.3 Radioactive exposure

To make sure that there is no risk to health due to radioactive exposure (radon) coming from the concrete tubes or the ground, The Institut fur Umwelt and Gesundheit (IUG) measured the air quality in an ETAHE. They did not state any increased values of Radon (^{220}Rn, ^{222}Rn) [Wagner, 2000].

2.6 Research needs

Determining the temperature variation in soil with the presence of an ETAHE is very important in that soil temperature around the tube is the key parameter affecting the performance of an ETAHE system. Also, potential condensation needs to be considered. However, there are no existing simple models to do such simulations. Meanwhile, designers need a simple method in sizing an ETAHE system. When designing, they want to estimate not only the outlet air temperature from the ETAHE but also the air relative humidity to choose the HVAC systems, through which outlet air will be further treated. This research work addresses these needs.

SOIL HEAT TRANSFER AND MODELING

3.1 Ground heat transfer mechanisms

The temperature field in the ground is influenced by different quantities (see Fig. 3.1.). Whereas the influence of trickling water or geothermal energy can probably be neglected [Wagner et al, 2000], the incoming solar radiation and the outgoing long wave radiation exchange between the ground and the sky have to be considered.
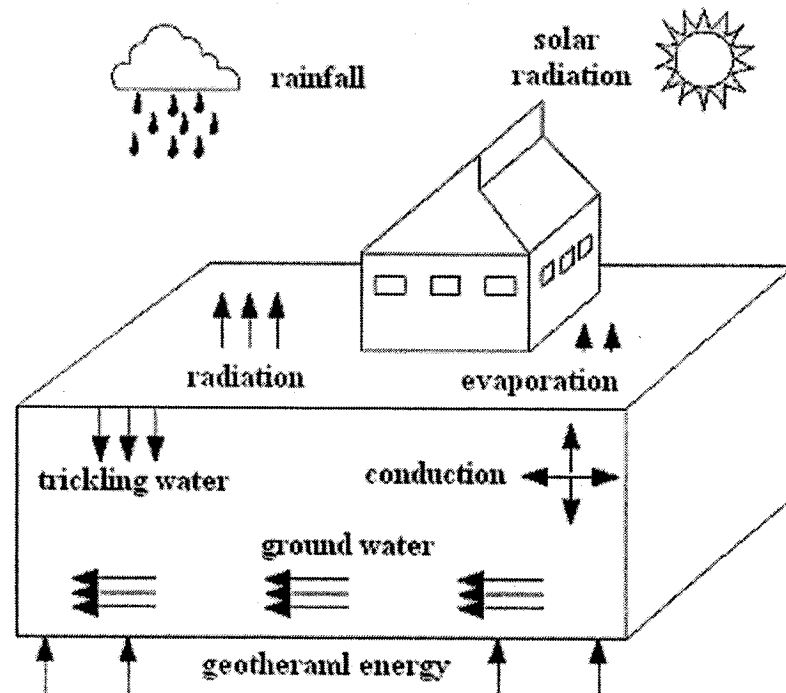
Fig. 3.1 Different environmental influences and heat transfer mechanisms that influence the temperature field in the ground [Wagner et al, 2000]

Absorption of the solar radiation depends on the ground cover and color, while the longwave radiant loss depends on soil surface temperature [Givoni, 1994]. The net

radiant balance between solar gain and long-wave loss is usually positive in summer and negative in winter. This causes heat to flow down from the surface into the ground in the summer and upward to the surface during the winter. The net radiant balance also determines the relationship between the averages of the earth surface and the ambient air temperatures. By shading the soil in summer while partially exposing it to the sky in winter, for example, with deciduous trees, it is possible to lower the ground temperature in summer to a greater extent while possibly increase the ground temperature in winter somehow.

Ground temperature (°C)

| -10 | -5 | 0 | 5 | 10 | 15 | 20 | 25 | 30 |

Depth (Meters)

2.0
4.0
6.0
8.0
10.0
12.0

Sod ground cover
is present
$k = 1.7$ W/m°C
Solid lines indicate
computer predictions
Symbols indicate
measured values

+ January
○ April
● July
● October
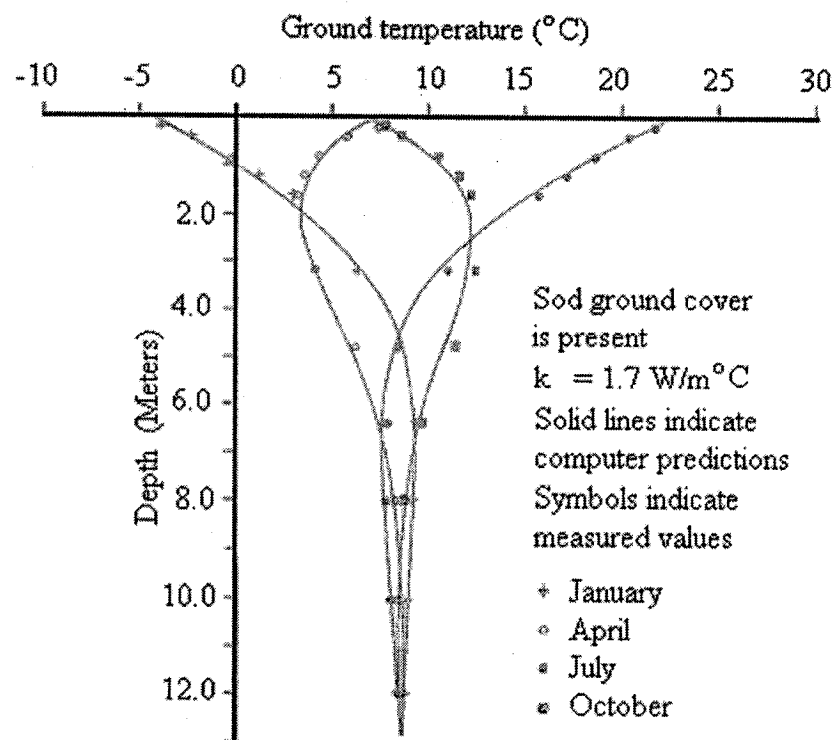
Fig. 3.2 Ground temperature variations as a function of depth [Carmody, 1985]

Changes in the Earth's surface temperature through time occur at several temporal scales. Figure 3.2 shows the ground temperature variations as a function of depth. The largest of these changes are the daily and seasonal variations, both of which can have

amplitudes of 10 $^\circ$C or more. Fortunately the Earth acts as a filter and attenuates these thermal waves with depth. The high frequency, or short term, variations die out more rapidly than long-term variations. Thus the daily temperature wave is barely observable below a depth of 1 m; the annual wave is not observable below 20 m. But the temperature at 1 m is an excellent, fully integrated average of the daily signal the previous day. Likewise, the temperature at 20 m is a proper measure of the integrated surface ground temperature over the previous annual wave. This integrating property makes the Earth a continuous and sensitive recorder of energy imbalances at the surface and of the small temperature differences associated with climate change.

3.2 Ground thermal properties

The performance of an ETAHE is directly related to the thermal properties of the ground. The ground has thermal properties that give it a high thermal inertia. The heat transfer mechanisms in soils are, in order of importance: conduction, convection and radiation. Conduction occurs throughout the soil but the main flow of heat is through the solid and liquid constituents. Convection is usually negligible, with the exception of rapid water infiltration after irrigation or heavy rain. Radiation is important only in very dry soils, with large pores, when the temperature is high. Therefore, the main parameters influencing the thermal behaviour of the soil are the thermal conductivity and heat capacity can be jointly expressed under the term of thermal diffusivity:

$$\alpha = \frac{k_s}{\rho_s c_s} \tag{3.1}$$

where k_s is the thermal conductivity, ρ_s the density and c_s the specific heat of the soil. Thermal diffusivity determines the thermal behavior of the soil.

28

The temperature field in the ground depends on the soil type and the moisture contained, respectively. In most cases there is not detailed information about soil characteristics available and the moisture varies throughout the year. However, ASHRAE (HVAC systems and equipment, 2000) gives the properties for number types of soil (see Table 3.1).

Table 3.1 Thermal properties of selected soils, rocks, and backfills (ASHRAE, 2000)

	Dry Density, kg/m^3	Conductivity, W/(m·K)	Diffusivity, m^2/day
Soils			
Heavy clay (15% water)	1925	1.4 – 1.9	0.042 – 0.061
Heavy clay (5% water)	1925	1.0 – 1.4	0.047 – 0.061
Light clay (15% water)	1285	0.7 – 1.0	0.055 – 0.047
Light clay (5% water)	1285	0.5 – 0.9	0.056 – 0.056
Heavy sand (15% water)	1925	2.8 – 3.8	0.084 – 0.11
Heavy sand (5% water)	1925	2.1 – 2.3	0.093 – 0.14
Light sand (15% water)	1285	1.0 – 2.1	0.047 – 0.093
Light sand (5% water)	1285	0.9 – 1.9	0.055 – 0.12
Rocks			
Granite	2650	2.3 – 3.7	0.084 – 0.13
Limestone	2400 – 2800	2.4 – 3.8	0.084 – 0.13
Sandstone	2570 – 2730	2.1 – 3.5	0.65 – 0.11
Wet shale		1.4 – 2.4	0.065 – 0.084
Dry shale		1.0 – 2.1	0.055 – 0.074
Grouts/Backfills			
Bentonite (20% soilds)		0.73 – 0.75	
Cement		0.70 – 0.78	
20% Bent.-40% SiO$_2$ sand		1.48	
Concrete (50% SiO$_2$ sand)		2.1 – 2.8	

Accurate knowledge of the soil thermal properties is very important for the design and the performance prediction of an ETAHE system. Goswami et al [1990] have set up experiments to investigate the thermal conductivity and the thermal diffusivity of the soil. The results showed that with a constant heat flux from a line source, the thermal

conductivity of the soil around the heat source decreases with time. This happens because of moisture movement in the soil away from the heat source, thereby reducing the thermal conductivity. When the heat source is turned off, the moisture slowly diffuses back, which then increases the thermal conductivity again. It was also shown that the amount of heat flux also affects the change in thermal conductivity. However, in this thesis we assumed constant thermal conductivity mainly for simplicity of the analysis because the thermal conductivity value tends to become steady after some initial period. This initial period depends on the heat flux. This may lead the small difference between theoretical prediction and experimental data that will be presented in Chapter 4.

The amount of heat conducted and how widely it is diffused varies from one soil type to another. The moisture content of the soil is a major influence on conductivity and diffusivity, and accounts for large variations on how heat moves through the earth. Soil thermal conductivity changes significantly with moisture content; for example, it was studied [ASHRAE] that soil thermal conductivity ranges from 0.14 W/(m·K) during dry soil conditions to 2.16 W/(m·K) during wet soil conditions. Figure 3.3 show how thermal conductivity varies as moisture in soil increases.

With the moisture content in soil considered, ASHRAE (HVAC systems and equipment, 2000) suggests using the following equation to calculate thermal diffusivity for soil:

$$\alpha = \frac{k_s}{\rho_s \left[c_s + c_w (w/100) \right]} \qquad (3.2)$$

where

c_s = dry soil specific heat, kJ/ (kg K)

c_w = specific heat of water = 4.18 kJ/ (kg K)

w = moisture content of soil, % (dry basis)

Because the specific heat of dry soil is nearly constant for all types of soil, c_s may be taken as 0.73 kJ/ (kg K)
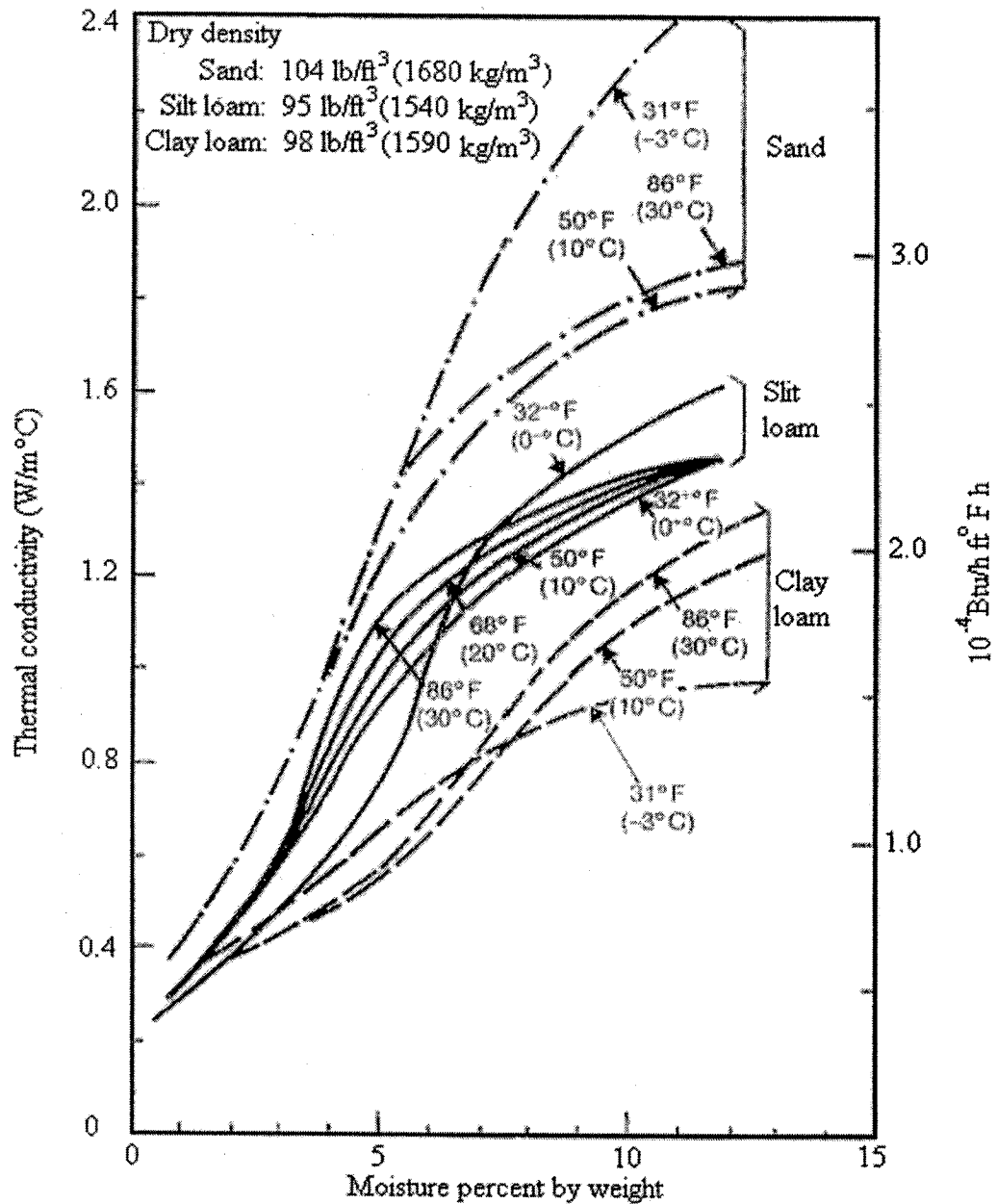
Fig. 3.3 Thermal conductivity of different soil as a function of moisture percent by weight [Labs, 1989]

31

3.3 Undisturbed ground temperature

In the design process, the undisturbed ground temperature is one of main input parameters. However, its accurate modeling is difficult because the soil parameters are often unknown. Additionally, the definition of "undisturbed ground temperature" is problematic due to the thermal influence of a building or different soil properties at an ETAHE. In the following, the undisturbed ground temperature is influenced by the building but not by the ETAHE and is defined for mean soil properties. Hence, the undisturbed ground temperature is a hypothetical value.

3.3.1 Modeling the ground temperature

The determinant parameter for the evaluation of the ground cooling and heating potential is the ground temperature at various depths. Ideally, this value should be measured. However, only a few weather stations perform measurements of ground surface temperature, while the number of the stations where measurements at various depths are performed is even smaller. This is why algorithms for the calculation of the ground temperature at various depths have been developed. For homogeneous soil of constant thermal diffusivity, the ground temperature at any depth z and time t is [ASHRAE--HVAC systems and equipment, 2000)]:

$$T(z,t) = T_m - A_s \exp\left[-z\left(\frac{\pi}{365\alpha}\right)^{1/2}\right]\cos\left[\left(\frac{2\pi}{365}\right)\left(t - t_0 - \frac{z}{2}\left(\frac{365}{\pi\alpha}\right)^{1/2}\right)\right] \quad (3.3)$$

where

T_m Average annual temperature of the soil surface (°C)

A_s Amplitude of surface temperature variation (°C)

z Depth (m)

α Thermal   diffusivity   of   the   ground (m^2/h)

t time elapsed from the beginning of the calendar year (hours)

t_0 A phase constant (hours) since the beginning of the year of the lowest

average ground surface temperature.

This equation shows that the soil temperature at a certain depth depends mainly on the

surface temperature and on the thermal characteristics of the soil. Table 3.2 shows

monthly soil temperature (1.5m) at major Canadian cities.

Table 3.2. Monthly ground temperatures (°C) (depth 1.5 meters). Source: "Soil temperature averages" from Atmospheric Environment Service

City	Jan	Feb	Mar	Apr	May	Jun	Jul	Aug	Sep	Oct	Nov	Dec	Ann
Vancouver	8.2	7.5	7.7	8.7	10.4	12.4	14.1	15.1	15.3	14.3	12.2	9.9	11.3
Edmonton	1.0	0.3	0.0	0.3	2.9	6.7	9.9	12.4	11.5	8.6	5.7	2.9	5.2
Regina	1.3	0.2	-0.2	-0.1	0.9	4.9	8.9	11.0	11.2	9.1	6.4	3.3	4.7
Winnipeg	2.9	1.6	0.9	0.8	1.8	5.4	9.5	12.1	12.5	10.9	8.1	5.1	6.0
Toronto	6.6	5.4	4.5	4.9	8.1	11.8	14.6	16.5	16.3	14.3	11.9	9.2	10.3
Montreal	3.3	2.3	1.4	1.4	4.2	8.2	11.3	12.9	13.2	11.2	8.4	5.4	6.9
Fredericton	4.4	3.3	2.8	2.6	5.1	9.1	12.1	13.7	13.8	12.0	8.7	6.0	7.8
St John's	4.2	3.2	2.7	2.5	3.9	6.8	9.7	11.6	11.7	10.3	8.2	6.1	6.7
Fort Smith	0.6	0.2	0.0	-0.2	-0.1	3.5	8.7	10.9	10.4	7.2	4.0	1.9	3.9

3.4 Modeling an ETAHE

3.4.1 Semi-infinite slab model

From the definition of thermal diffusivity and the values in Table 3.1, it is concluded

that heat tends to be stored in the ground, rather than to propagate in it. Ground can be

considered as a semi-infinite medium and therefore the heat transfer equation becomes

$$\frac{\partial T}{\partial t} = \alpha \frac{\partial^2 T}{\partial z^2}$$ (3.4)

Although it is not an exact representation of real situations considering heat transfer to the ground as heat conduction in a semi-infinite slab, it can provide preliminary estimates, which may be used to validate more detailed numerical models [Athienitis, 1998].

A semi-infinite slab is a model for a body with a single plane surface (x=0) and its other surfaces distant enough to ignore for time periods of interest in transient analysis. If a uniform boundary condition is applied at $x = 0$, it is reasonable to assume that this case can be analyzed as transient one-dimensional conduction. One case that closely fits this model is the ground, with a uniform surface or air temperature; if we measure the soil temperature deep into the ground away from the surface, one would expect that the temperature is not significantly affected by what is happening at the surface. We have three main boundary conditions:

Case 1: Ambient temperature T_a at $z = 0$ imposed at time $t = 0$ with initial uniform body temperature T_s. The solution is given by:

$$T(z,t) = T_s + (T_a - T_s) \times erf\left[z / 2(\alpha t)^{1/2}\right]$$ (3.5)

Case 2: Convective boundary condition h at $z = 0$, environment temperature T_a and initial ground temperature T_s:

$$T(z,t) = (T_a - T_s) \times \left[1 - erf\left(\frac{z}{2\sqrt{\alpha t}}\right) - \exp\left(\frac{hz}{k} + \frac{h^2 \alpha t}{k^2}\right)\left(1 - erf\left(\frac{z}{2\sqrt{\alpha t}} + \frac{h\sqrt{\alpha t}}{k}\right)\right)\right] + T_s$$ (3.6)

The heat flow at the surface at time t is given by

$$q = h_s (T_a - T_s) \times \exp\left(\frac{h^2 \alpha t}{k^2}\right) \times \left[1 - erf\left(\frac{h\sqrt{\alpha t}}{k}\right)\right] \tag{3.7}$$

Case 3: Assuming that ground surface is subjected to a sinusoidal variation, then the boundary conditions are

$$T(t,0) = T_a + A_0 \cos \omega t \tag{3.8}$$

where T_a is the ambient air temperature, A_0 is the amplitude of the assumed sinusoidal variation and ω is angular frequency of the variation (s^{-1}).

The solution of equation is

$$T(z,t) = T_a + A_0 e^{-z/d} \cos\left(\omega t - \frac{z}{d}\right) \tag{3.9}$$

where $d = (2\alpha/\omega)^{0.5}$ is called the damping depth, because it governs the penetration depth of the 'temperature waves' in the soil. At a depth of 5d, the temperature variations are almost completely damped out.

Simulation results (Appendix A) show that rapid temperature variations, such as the daily variation of the ambient temperature, have a small damping depth and therefore, below a depth of 2m, the ground temperature is not influenced [Athienitis, 1998]. This is the physical principle on which an ETAHE is based.

3.4.2 Thermal network model

In order to calculate the dynamic temperature variation within the ground with the presence of an ETAHE, transient thermal analysis of soils should be performed. Athienitis et al [2002] described a control volume thermal network approach for transient thermal analysis of buildings. The same approach may be applied here. The soil around a

tube is divided into a number of layers. Each layer is represented by a node (Figure 3.4).

Each node i has a thermal capacitance C_i associated with it and resistances connecting

to adjacent nodes. Connecting these nodes with the resistances and capacitances, a

thermal network is constructed (Figure 3.5). This approach is based on the following

assumptions:

a. The influence of the ground surface temperature is ignored.

b. The heat flux is allowed in only the radial direction. Each layer is isothermal.

c. Initially, both air and ground temperatures are at the undisturbed ground temperature T_g.

d. At a radial distance of r_i, the ground temperature is at T_g. This r_i is investigated through simulation.

An energy balance is applied at each node at regular time intervals to obtain the

temperature of the nodes as a function of time. These energy balance equations for all

nodes may be solved with the explicit method in which we march forward in time from a

set of initial conditions.

The general form of the explicit control volume formulation corresponding to node

i and time interval p is:

$$T_{i,p+1} = \frac{\Delta t}{C_i} \times \left(Q_i + \sum \frac{T_{j,p} - T_{i,p}}{R_{i,j}} \right) + T_{i,p} \qquad (3.10)$$

where

36

$$C_i = \pi L \left[(r_i)^2 - (r_{i-1})^2 \right] \rho c \qquad (3.11)$$

subscript i indicates the node for with the energy balance is written and j all nodes connected to node i, while p is the time interval; Q_i represents a heat source at node i. The thermal resistance of the tube and any concentric circular soil layer is given by (Holman, 2002):

$$R_i = \frac{\ln\left(\dfrac{r_i}{r_{i-1}}\right)}{2\pi k L} \qquad (3.12)$$

The time step was selected based on the following condition for numerical stability:

$$\Delta t \leq \min\left(C_i / \sum_j \frac{1}{R_{i,j}} \right) \quad \text{for all nodes } i \qquad (3.13)$$

Simulations were performed in the environment of MathCAD 2001i (Appendix B). As shown in the program, we consider an ETAHE with a diameter of 0.5m. We assume that the ground temperature far from the tube remains equal to the undisturbed soil temperature. Ground in between is divided into 100 layers, the thickness of the layers near the tube are smaller than that far away from the tube.

Figure 3.6 show that temperature field beyond 2m from the ETAHE is basically not affected by the presence of the tube. Moreover, the ground temperature near the ETAHE increases only by around 2°C after 10 hours, which is the typical operating time for many commercial buildings. Figure 3.7 shows that heat flow rate approaches constant after 10 hours indicating the heat transfer reaches steady-state by then.
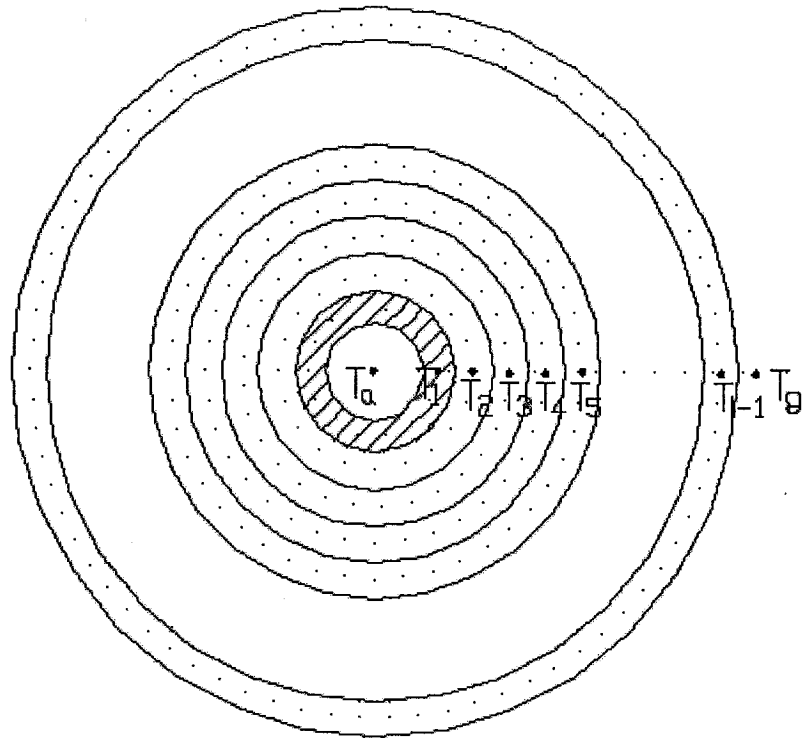
Fig. 3.4 Spatial discretization and node configurations
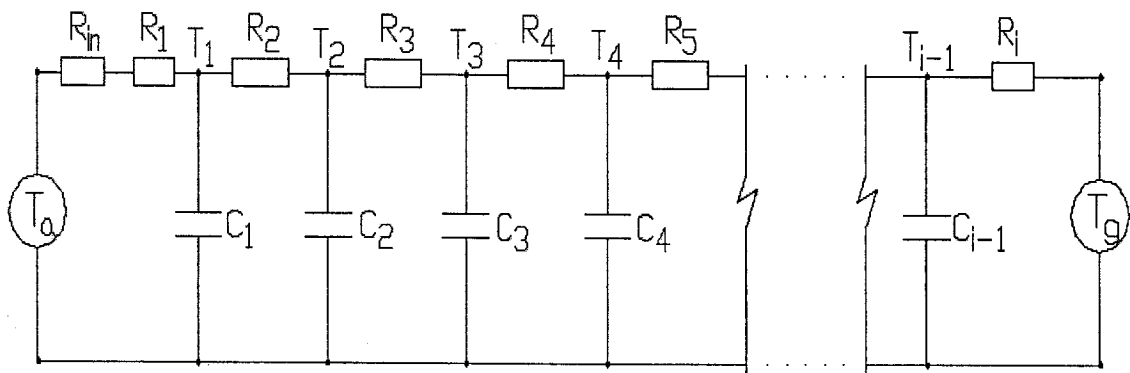
Fig. 3.5 Thermal network for soil around an ETAHE

38
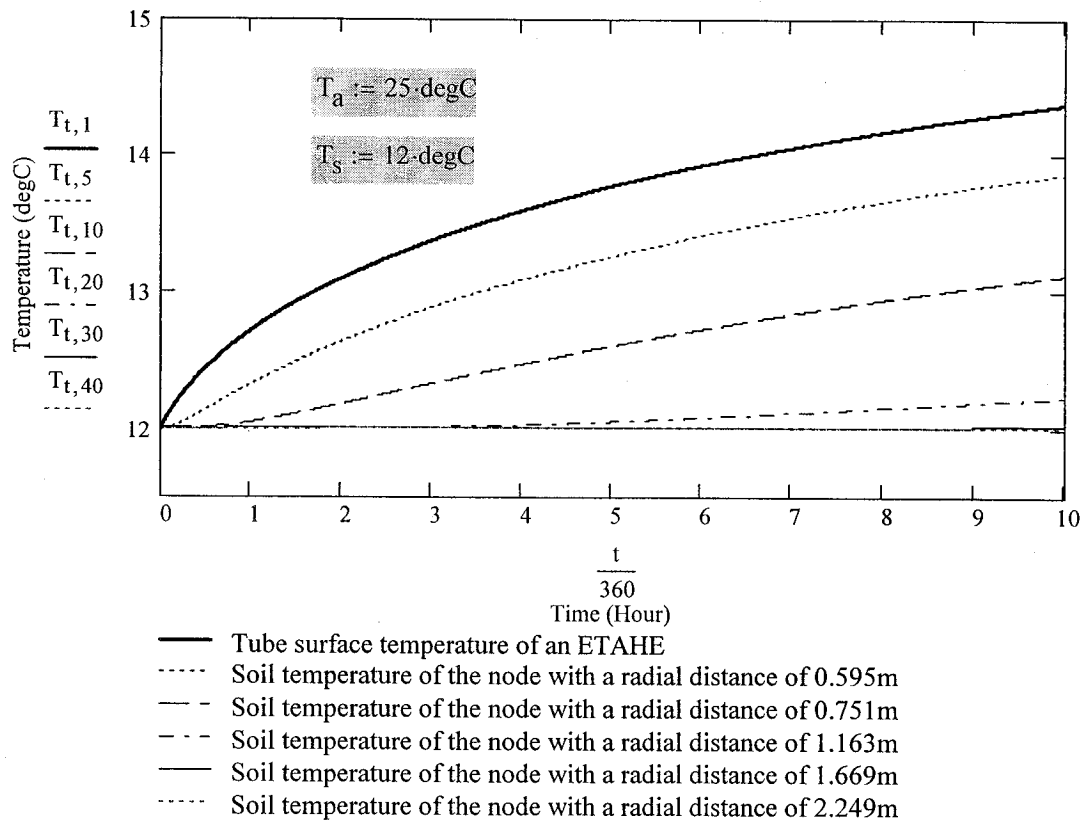
Fig. 3.6 Ground temperature at different radial distances as a function of time
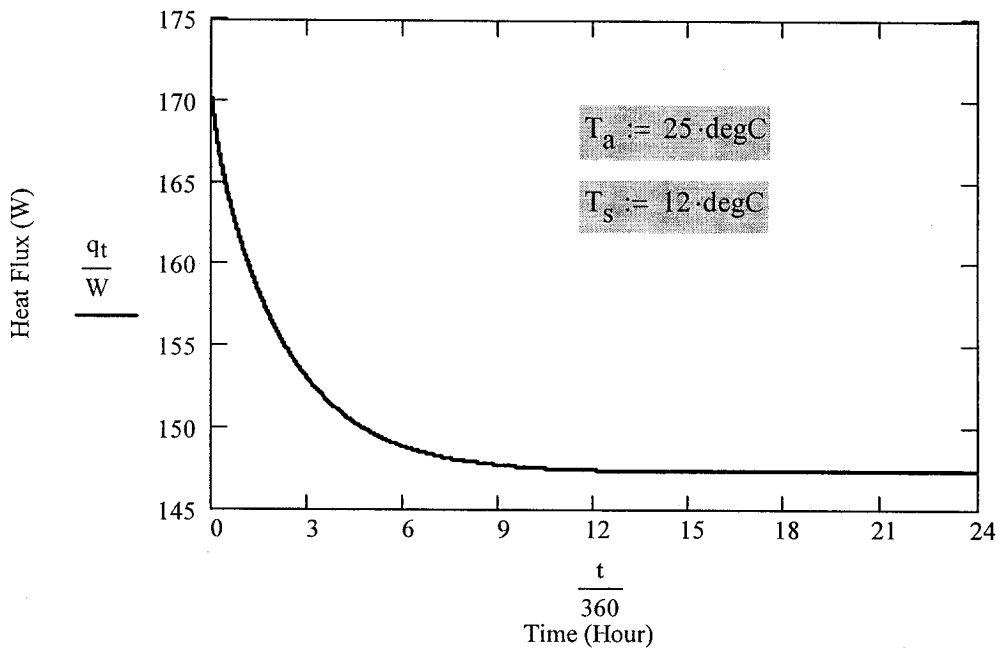
Fig. 3.7 Heat flow from the ETAHE to the soil

CHAPTER 4

SIMULATION OF AN EARTH-TO-AIR HEAT EXCHANGER

4.1 Introduction

In most cases the ETAHE is just one component in a whole building system. Designers do not have much freedom of choice to determine the size and layout of the ETAHE. They are limited by space-constraints and economic considerations. They need a simplified way to predict the general performance of the heat exchanger. Their main concern is to be able to select a reasonable size of the tube diameter, tube length and number of tubes. The most important question is whether adding another tube or another meter to the tubes will result in economic performance amelioration. A simple 1-D steady-state methodology may meet those needs. In this chapter, a control volume method will be presented to study the performance of an ETAHE.

4.2 Methodology

4.2.1 An analytical model

This model [Athienitis et al, 2002] is based on the following assumptions:

a. The ETAHE is of uniform cross-section.

b. The soil properties are isotropic.

c. There exists a perfect contact between the soil and the tube.

d. Thermal resistance due to tube thickness is negligible.

e. Ground is dry and heat transfer by moisture gradients in the soil is neglected.

f. Air is supposed to be incompressible and its thermal properties are kept constant

for calculations.

g. Heat extraction does not disturb the temperature distribution of the surrounding soil. The temperature of the tube surface is undisturbed ground temperature.

Assumptions a to f are made for simplification. Assumption g is based on the simulation results in Chapter 3 that the tube surface temperature varies by no more than 2°C after 10 hours' continuing operation. Goswami et al [1990] also did some temperature measurements along a tube surface. Experimental results show that the surface temperature varies by not more than 2°C except near the inlet and outlet. Near the inlet and outlet the surface temperature gets modified due to heat exchange of the end surfaces with the ambient. According to the assumptions, the heat will mainly be transferred by convection. Normally, an ETAHE system seldom operates continually for more than 6 hours in that the beneficial temperature difference between ambient air and undisturbed ground is unable to maintain so long.
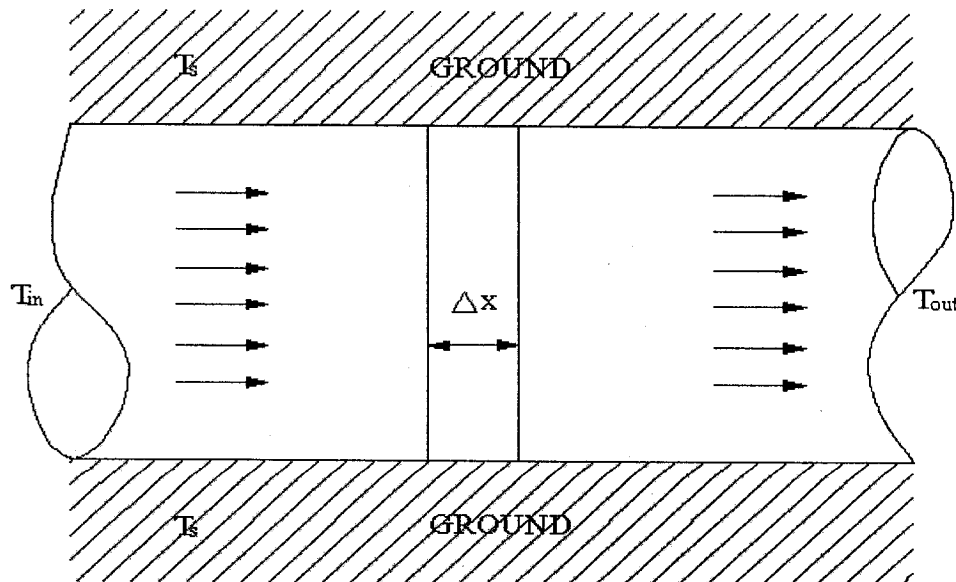
Fig. 4.1 Energy balance in an infinitesimal element

Then, let us consider an infinitesimal element of tube in the direction of air flow (Figure 4.1). T_s, the surface temperature of the tube, is assumed to be greater than the inlet air temperature.

The energy balance over this element of width dx may be written as

$$\dot{m}C_a dT_a = A_p f_a h_c (T_s - T_a) dx \qquad \text{(4.1)}$$

where

h_c is the convective heat transfer coefficient

T_s is the tube soil surface temperature (assumed constant)

T_a is the air temperature as a function distance from the tube inlet

A_p is the tube perimeter

$\dot{m}$ is the air flow rate

Thus, the differential equation can be written as:

$$a\frac{d\theta}{dx} + \theta = 0 \qquad \text{(4.2)}$$

where

$$\theta = T_a - T_s \qquad \text{(4.3)}$$

$$a = \frac{\dot{m}C_a}{A_p h_c f_a} \qquad \text{(4.4)}$$

f_a is factor considering heat transfer enhancement by using corrugated tube or by adding vertical fins. The heat transfer coefficient at the inner surface of the tube h_c depends on flow properties, dimensions of the tube and air properties:

$$h_c = \frac{k_{air} Nu}{D} \qquad \text{(4.5)}$$

The Nusselt number Nu of air in a tube depends on Reynolds number Re and thus on flow rate. For turbulent airflow in the temperature region (-30° to 30°) relevant for the ETAHE, we use the following Dittus-Boelter correlation as approximation (Holman 2002):

$$Nu = 0.023\,\text{Re}^{0.8}\,\text{Pr}^{0.3} \quad \text{when cooling} \tag{4.6}$$

$$Nu = 0.023\,\text{Re}^{0.8}\,\text{Pr}^{0.4} \quad \text{when heating} \tag{4.7}$$

Where Nu is Nusselt number, Re is Reynolds number and Pr the Prandtl number for air (typically: $\text{Pr} = 0.7$).

On solving the above ordinary differential equation (4.2) in combination with the initial condition, that

$$T_a = T_o \quad at \quad x = 0 \tag{4.8}$$

One gets

$$T_a(x) = T_s - (T_s - T_o)\exp(-x/a) \tag{4.9}$$

The rise in tube air temperature may then be calculated by the expression

$$\Delta T = (T_s - T_o)[1 - \exp(-L/a)] \tag{4.10}$$

where L is the length of the tube. It is obvious with this expression that if the inlet air temperature is higher than the surface temperature of the tube, a negative ΔT will be obtained indicating that the air is being cooled.

The 1-D model (Appendix C) gives an exact solution to the ETAHE problem. However, it cannot predict condensation rate that may happen in summer time.

4.2.2 A control volume model

In order to develop a simple 1-D model, which can predict both outlet temperature and

43

relative humidity, the tube is divided into a large number of elements (Figure 4.2).

Energy balance is made on each element (Figure 4.3).
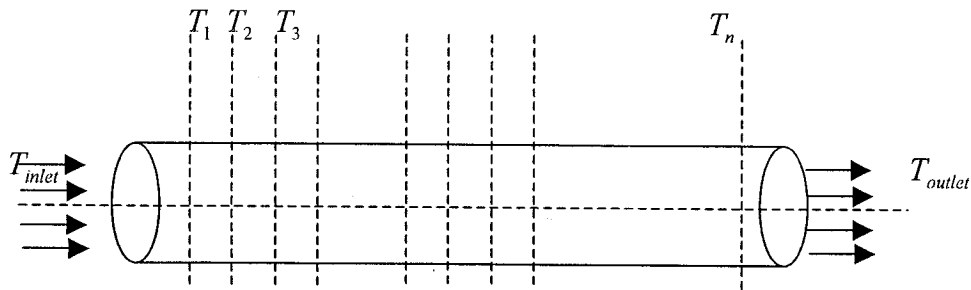
T_n -- Outlet Temperature for Element n

Fig. 4.2 Calculation of the temperature of the air at any point in the tube buried
underground by a control volume method
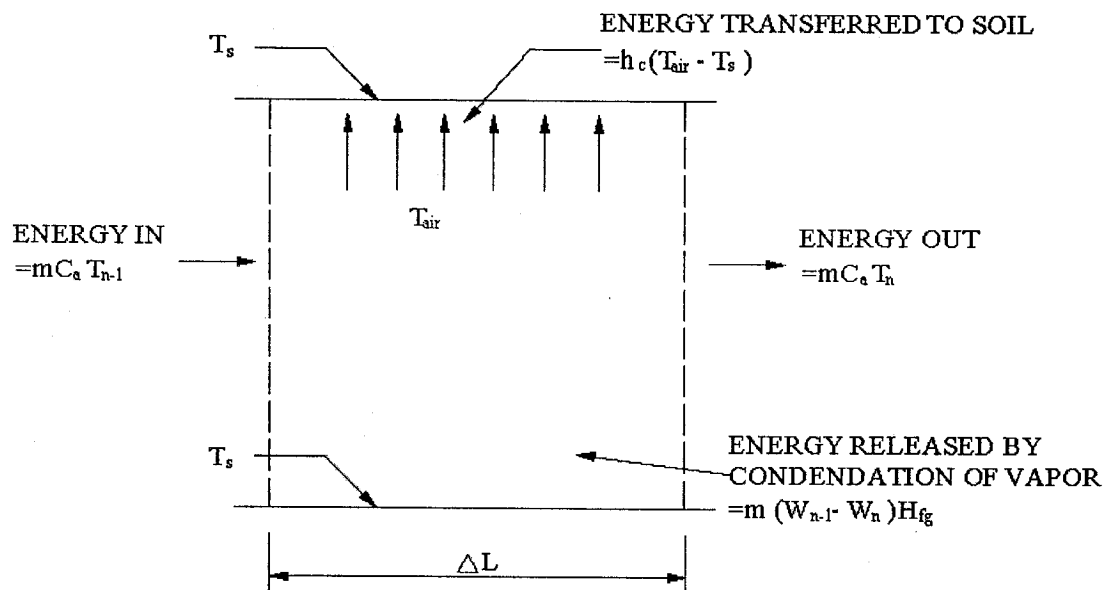
Fig. 4.3 Energy balance in an element

Assumptions are the same as those in the analytical model. To analyze the heat transfer

from air to the tube, we solve it in two different cases:

1. If the tube surface temperature is higher than the dew-point temperature of the inlet

44

air entering an element, there will be no condensation. The energy balance is:

$$\dot{m}C_{air}\left(T_{n-1}-T_n\right)=h_cA_p\left(T_{air}-T_s\right) \tag{4.11}$$

Here, we may apply the analytical solution when we calculate T_{air}. Divide each element into i sub-elements; assume there is no condensation in each sub-element. According the analytical solution, we get average air temperature in each element as follows:

$$T_{air}=\frac{\sum\limits_i\left[T_s+\left(T_{n-1}-T_s\right)e^{-Xi/a}\right]}{i} \tag{4.12}$$

Substituting in (4.11) and simplifying we obtain:

$$T_n=T_{n-1}-a\left(\frac{\sum\limits_i\left[T_s+\left(T_{n-1}-T_s\right)e^{-X_i/a}\right]}{i}-T_s\right) \tag{4.13}$$

2. If the tube surface temperature is lower than the dew-point temperature of the inlet air entering an element, not only will the temperature of the air change but moisture will also be condensed out of the air. The mass balance equation for this process is,

$$\dot{m}\left(W_{n-1}-W_n\right)=h_mA_p\rho_a\left(W_a-W_s\right) \tag{4.14}$$

For turbulent flow through a tube, the convective mass transfer coefficient can be obtained by Lewis relation [ASHRAE, 2001]:

$$h_m=\frac{h_c}{\rho_ac_a} \tag{4.15}$$

Energy balance equation is:

$$\dot{m}C_{air}\left(T_{n-1}-T_n\right)+\dot{m}\left(W_{n-1}-W_n\right)H_{fg}=h_cA_p\left(T_{air}-T_s\right) \tag{4.16}$$

Combining equations (4.11), (4.12), and (4.16), we can obtain T_n and W_n. Because air

Input geometrical properties of the ETAHE (diameter D and length L)
Input inlet air temperature (t_o), relative humidity (RH_o) and velocity (V)
Input soil temperature (t_s)

Divide the tube into 50 control volumes, each volume into 10 elements. Input both air and soil property parameters

Calculate Reynolds number (Re) then find convective heat transfer coefficient (h_c) according to Dittus-Boelter Relation and mass transfer coefficient (h_m) according to Lewis Relation

Determine the coefficients U and a in two heat balance equations

Calculate average air temperature (T_{air}) in each control volume according to the analytical model

Determine if the tube surface temperature is lower than the dew point of air in each control volume

Yes

No

Condensation occurs

No condensation

Apply both heat and mass balance

Apply only heat balance

Find air temperature and RH when leaving each element
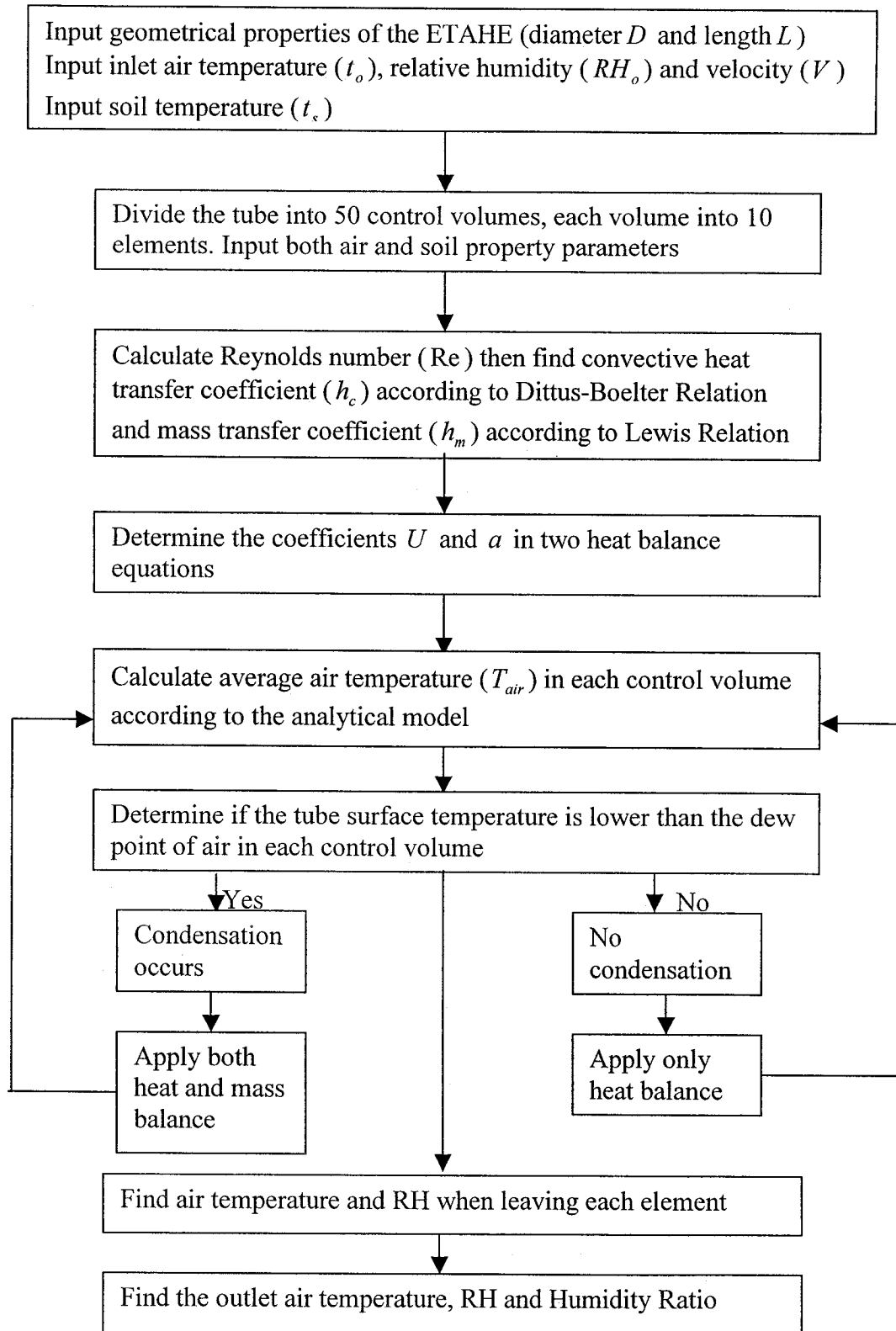
Find the outlet air temperature, RH and Humidity Ratio

Fig. 4.4 The flow chart of the method developed to simulate the ETAHE

relative humidity is the function of air temperature and its humidity ratio, we can get the outlet air temperature and RH by performing iterations. This model will usually overpredict condensation especially for large tubes because some of the air may not come into contact with the tube surface. CFD studies are needed to study this in more detail.

The program (Appendix D) is developed in MathCAD 2001i. Its algorithm is summarized in Figure 4.4. By using the tube surface temperature obtained from the thermal network program in Chapter 3, we may find the outlet air temperature considering the soil temperature variation influenced by the presence of the ETAHE. Appendix E also gives a program to calculate fan power needed and system COP.

4.3 Simulation results

Simulations are carried out to demonstrate the performance of an ETAHE with a length of 50m and a diameter of 0.5m. The air velocity inside the tube was assumed to be a constant 2m/s. Both heating and cooling cases are studied.

4.3.1 A heating case

In a heating case, we assume the outdoor air temperature is -5°C, relative humidity 40%, and undisturbed soil temperature 12°C. Figure 4.5a, Figure 4.5b, Figure 4.5c illustrate that the air temperatures, air relative humidities and air humidity ratios vary along the ETAHE. As can be seen from the three figures, air temperature is increased 15°C from -5°C to 10°C. In the meantime, air relative humidity drops from 40% to14% while humidity ratio remains constant. By trying different input parameters, we conclude that the preheating potential is great in the wintertime using such a system. But one of its

main disadvantages is that the air relative humidity is lowered to an unfavorable level. Humidification must be applied.

4.3.2 A cooling case

For cooling use of the same ETAHE, we assume outdoor air temperature is 30°C, relative humidity 70%, and undisturbed soil temperature 12°C. Figure 4.6a, Figure 4.6b and Figure 4.6c illustrate that the air temperatures, air relative humidities and air humidity ratios vary along the ETAHE with an inlet. As can be seen from the three figures, air temperature drops 16°C from 30°C to 14°C. In the meantime, air relative humidity rises from 70% to 89%, meanwhile condensation occurs within the first 24m of the tube with a rate of 4kg/hr.

By trying different input parameters, we conclude that the cooling potential is also great in the summer time using such a system. But one of its main disadvantages is that the air relative humidity is handled to an unfavorable level. Dehumidification must be applied.
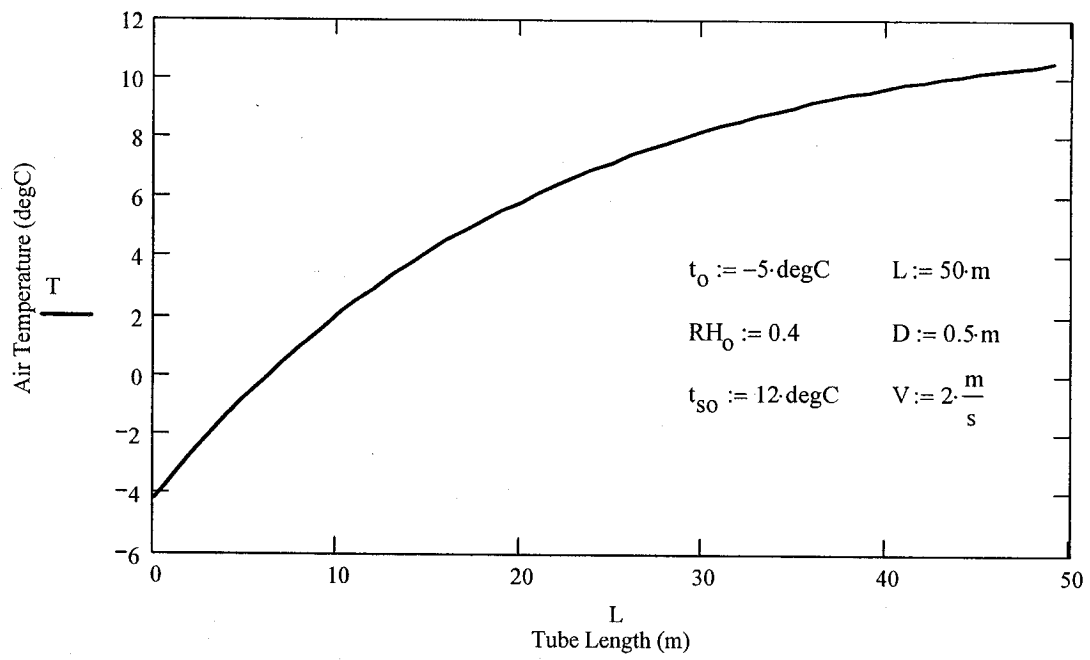
Fig. 4.5a A heating case: air temperature varies along an ETAHE
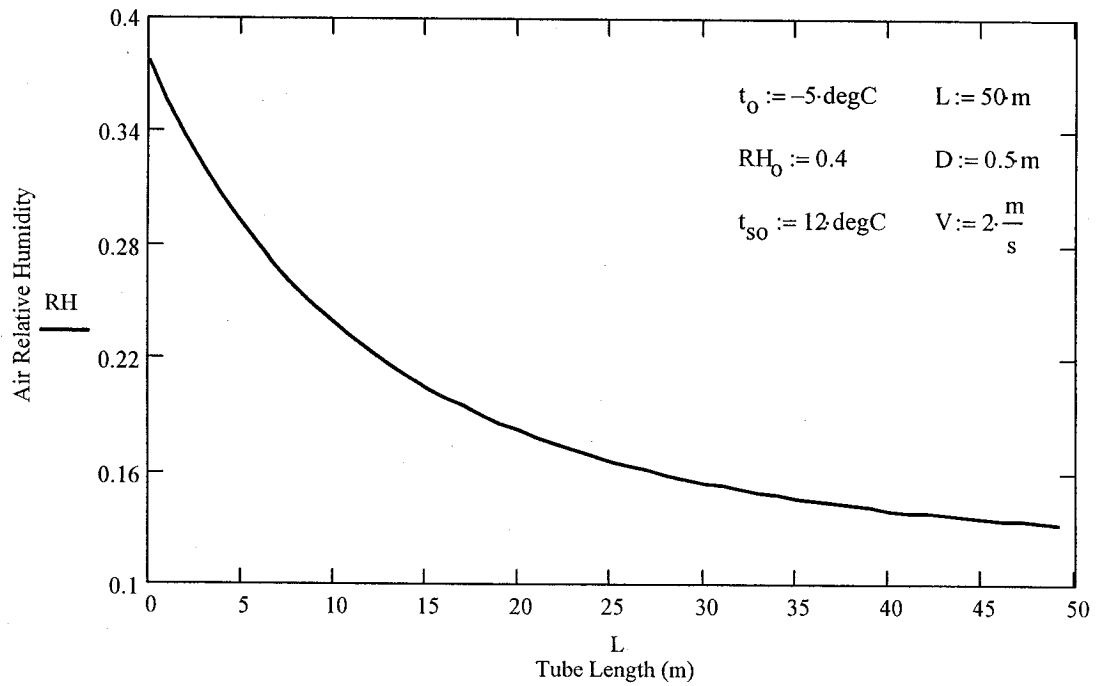

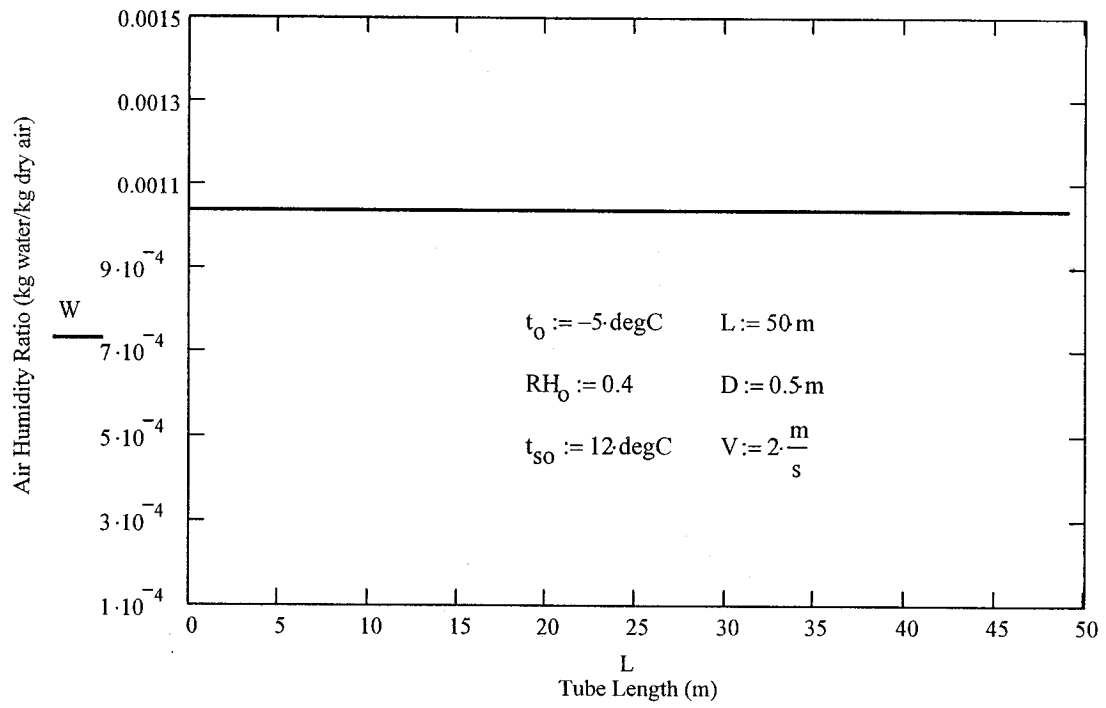Fig. 4.5b A heating case: air RH varies along an ETAHE

49

Fig. 4.5c A heating case: humidity ratio varies along an ETAHE
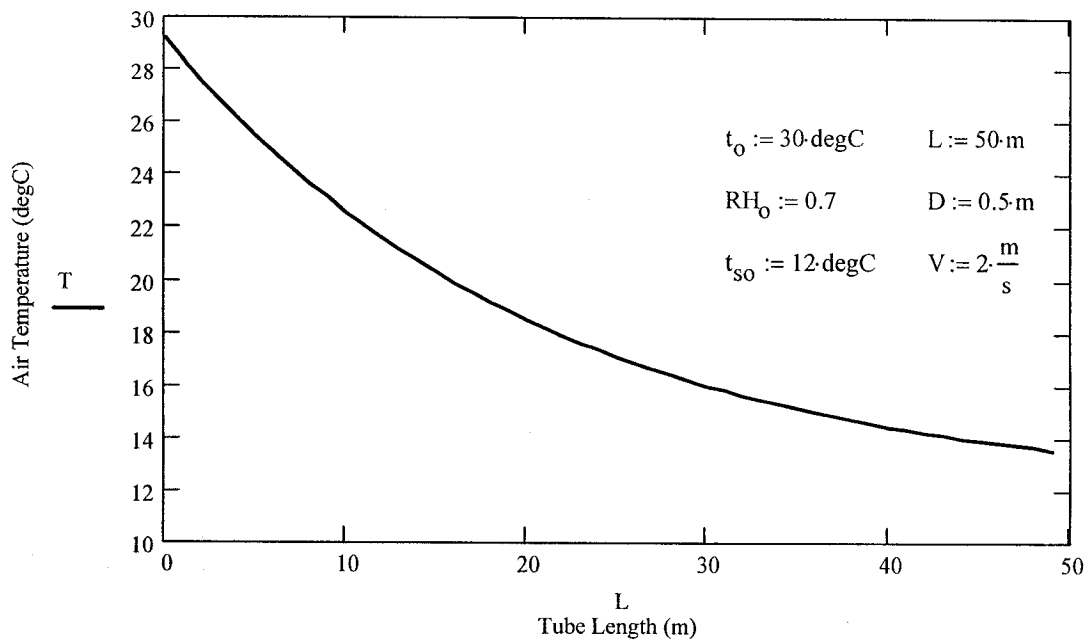

Fig. 4.6a A cooling case with condensation: air temperature varies along an ETAHE
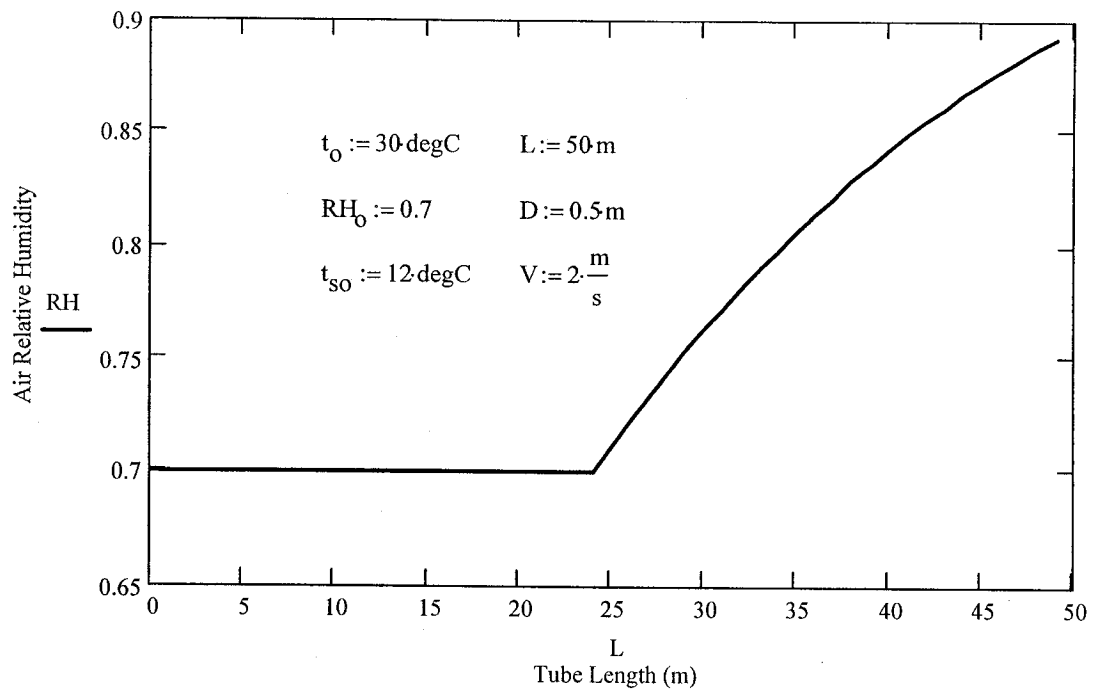
50

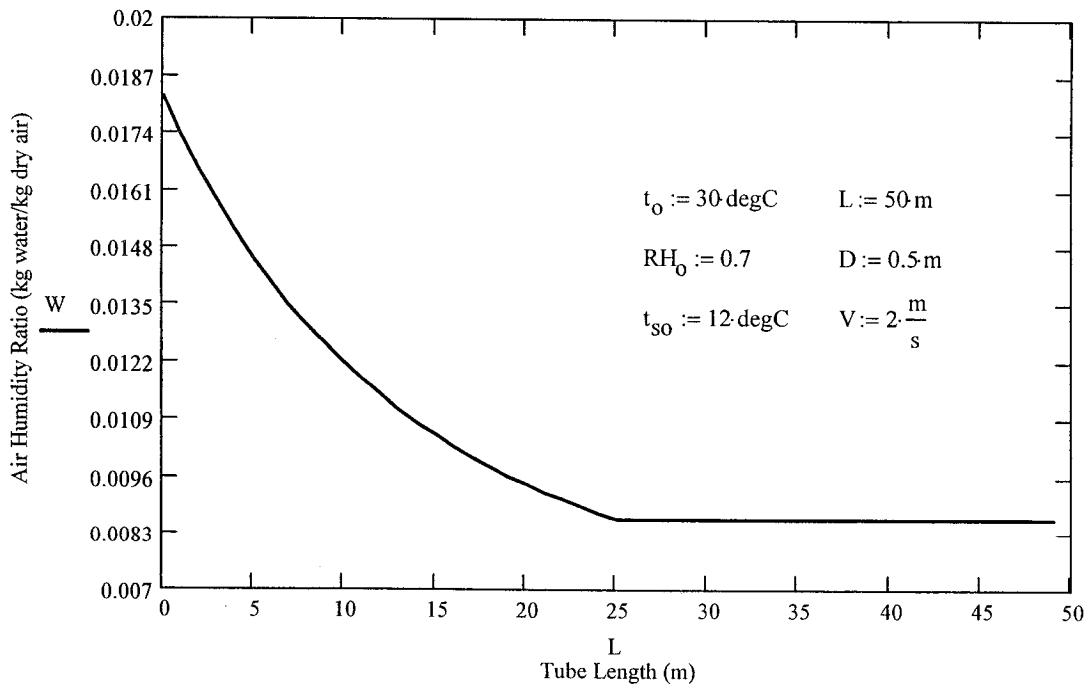Fig. 4.6b A cooling case with condensation: air RH varies along an ETAHE

Fig. 4.6c A cooling case with condensation: humidity ratio varies along an ETAHE

51

4.4 Model validations

In order to evaluate and validate the algorithms discussed above, two sets of published experimental data are compared with simulation results.

4.4.1 Validation with Goswami's experimental data

Goswami et al [1990] obtained the first experimental data. The experiments were performed at outdoor environmental study laboratory at the N.C. A&T State University. A corrugated plastic tube of 0.3m in diameter and 25m in length was buried in the soil at about 2.1m to 2.4m in depth. The experiment site was a mixture of clay, sand and small rocks. Temperature of air, tube surface, and soil at different locations were measured using iron-constantan thermocouples. The temperature of the air and the tube surface were measured at distances of 0.3, 3.4, 6.4, 9.5, 12.5, 15.6, and 24.7 from the inlet end. Air velocity in the tube was measured about 0.3m from the entrance. To minimize errors, air velocity was measured at several points on two different diameters and then averaged.

Simulation is carried out using these inputs. Figure 4.7 compares the air temperatures in the tube with theoretical predictions. It can be seen from the figure that the agreement between the experimental data and the theoretical results is reasonably good. Various sources of error that may contribute to the differences between the experimental and the theoretical values include air velocity measurements and heat transfer enhancement due to the corrugated tube.
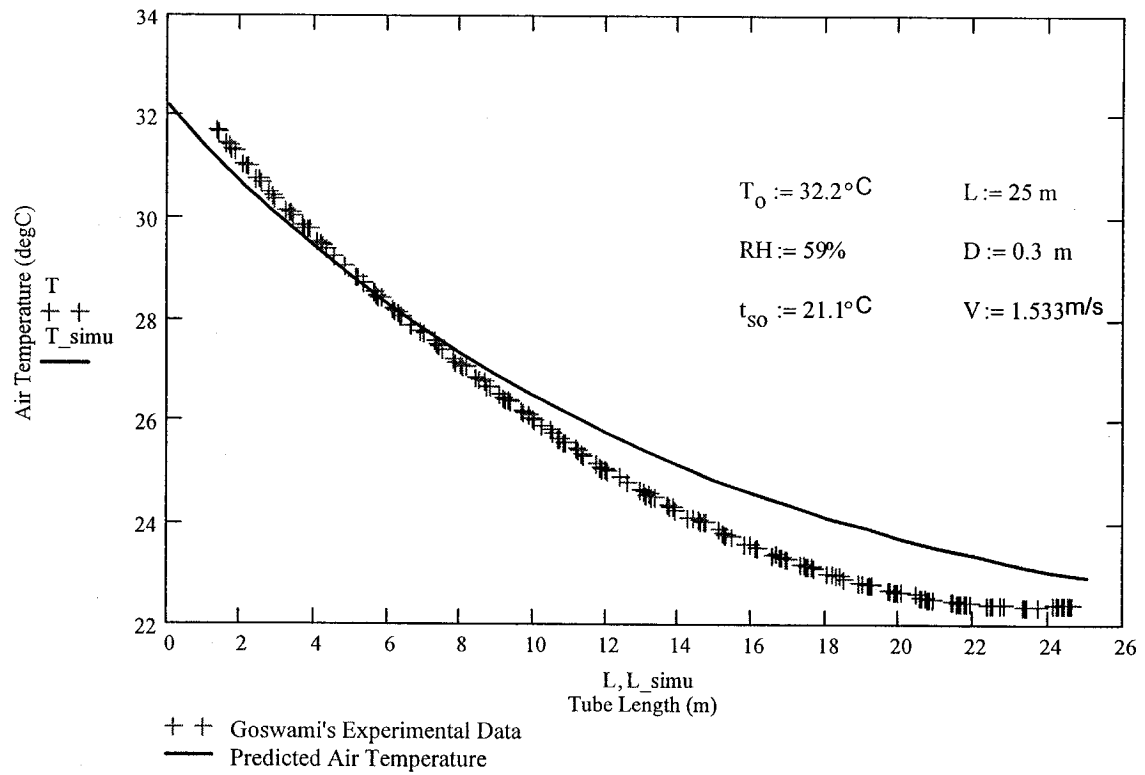
Fig. 4.7 Simulation results compared with Goswami's experimental data

4.4.2 Validation with Benkert's experimental data

The second set of experimental data was measured by Albers to investigate the performance of an ETAHE for a warm summer day as referred by Benkert [1998]. The parameters for the model were chosen to represent the real weather conditions at the time of measurement, e.g. inlet air temperature was 25.3°C, and undisturbed ground temperature was 12.8°C as indicated in the upper left corner of Figure 4.8.

Again, the predicted results and the experimental data agree with each other well. The discrepancy of the temperatures may be explained by inhomogeneous soil prosperities around the real ETAHE whereas the model assumes fixed values.
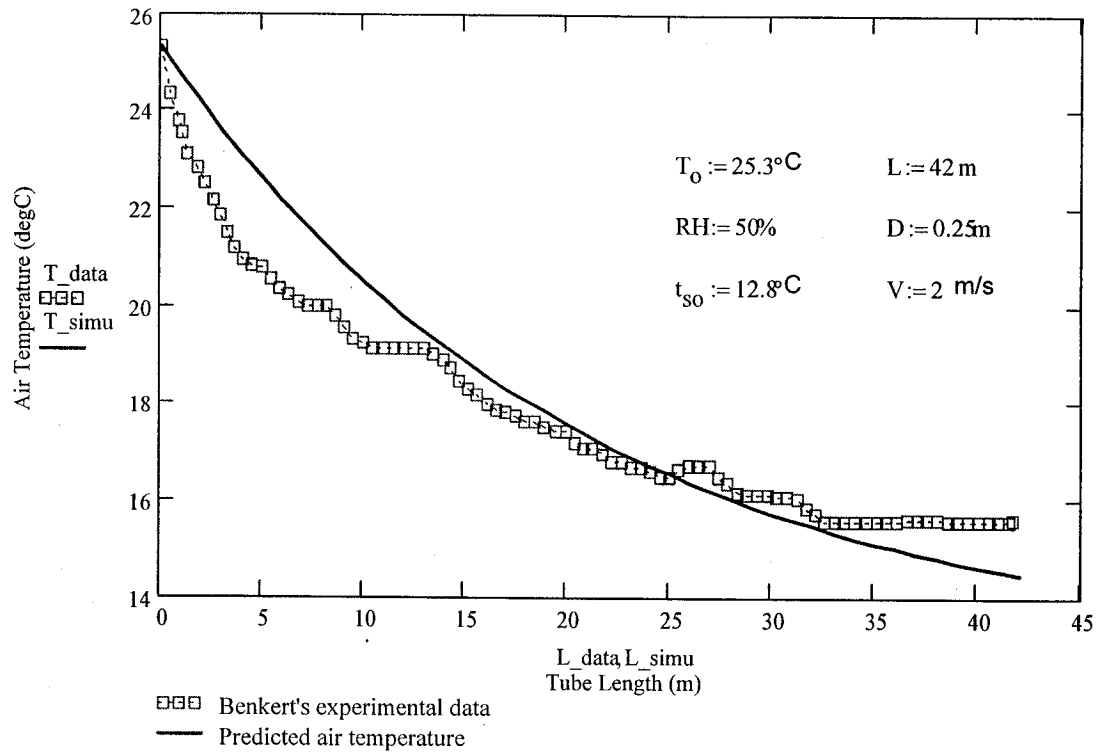
Fig. 4.8 Simulation results compared with Benkert's experimental data

4.5 Sensitivity analysis

A sensitivity analysis was carried out in order to identify the dominant design parameters. Figure 4.9 to Figure 4.13 show the variation of the air temperature as a function of the tube length when one of inputs varies.

Figure 4.9 shows the variation of the air temperature as a function of the tube length at inlet air temperatures 25°C, 27°C, and 30°C, respectively. Other necessary input data are shown in upper left corner of the Figure 4.9. The outlet air temperature is not sensitive to inlet air temperature variation. From these curves, we find the outlet air temperature will

54

change very little after a particular tube length. So an optimal tube length does exist. In this case, a 50m tube is long enough when we only expect a good outlet air temperature. There will be no further benefit if we use a much longer tube.

Figure 4.10 shows the variation of the air temperature as a function of the tube length at inlet air RH of 70%, 40%, and 20%, respectively. Other necessary input data are shown in upper left corner of the Figure 4.10. Literally, we find only one curve in the figure because the three curves are nearly fit together. We can make such a conclusion that latent heat is so small compared with sensitive heat that it can be neglected.

Figure 4.11 shows the variation of the air temperature as a function of the tube length at undisturbed ground temperatures of 17°C, 14°C, and 12°C, respectively. Relevant input data are shown in upper left corner of the Figure 4.11. From these curves, we may infer that the deeper the tube the better the outlet air temperatures.

Figure 4.12 depicts the variation of the air temperature as a function of the tube length at tube diameters of 0.5m, 0.4m, and 0.3m, respectively. Other necessary input data are shown in upper left corner of the Figure 4.12. Results show that a smaller tube diameter is better than a larger one. Choosing a small diameter tube will definitely lower capital costs. On the other hand, a smaller diameter tube will lead to more power consumption because of an increased resistance. Hence, an optimal size has to be obtained taking into account all factors.

Figure 4.13 shows the variation of the air temperature as a function of the tube length at air velocity of 3m/s, 2m/s, and 1m/s, respectively. Other necessary input data are

shown in upper left corner of the Figure 4.13. Results show that a lower flow rate makes

the air temperature drop more quickly than a higher one.
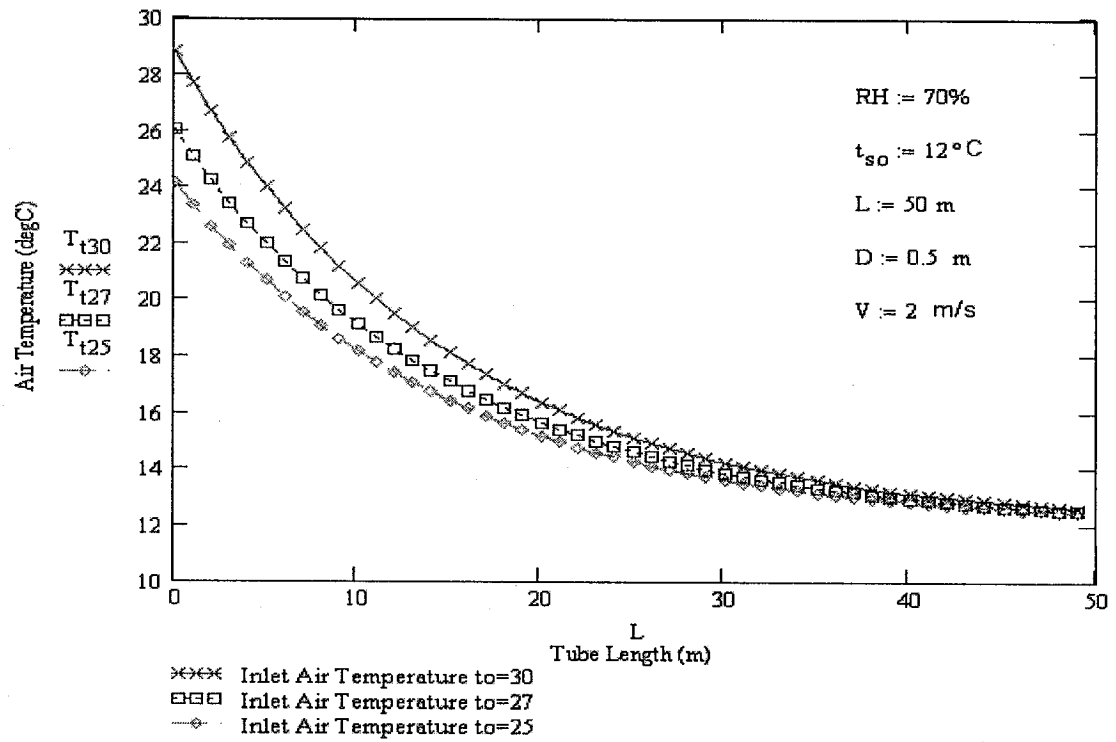

Fig. 4.9 Air temperature inside an ETAHE at different inlet air temperature
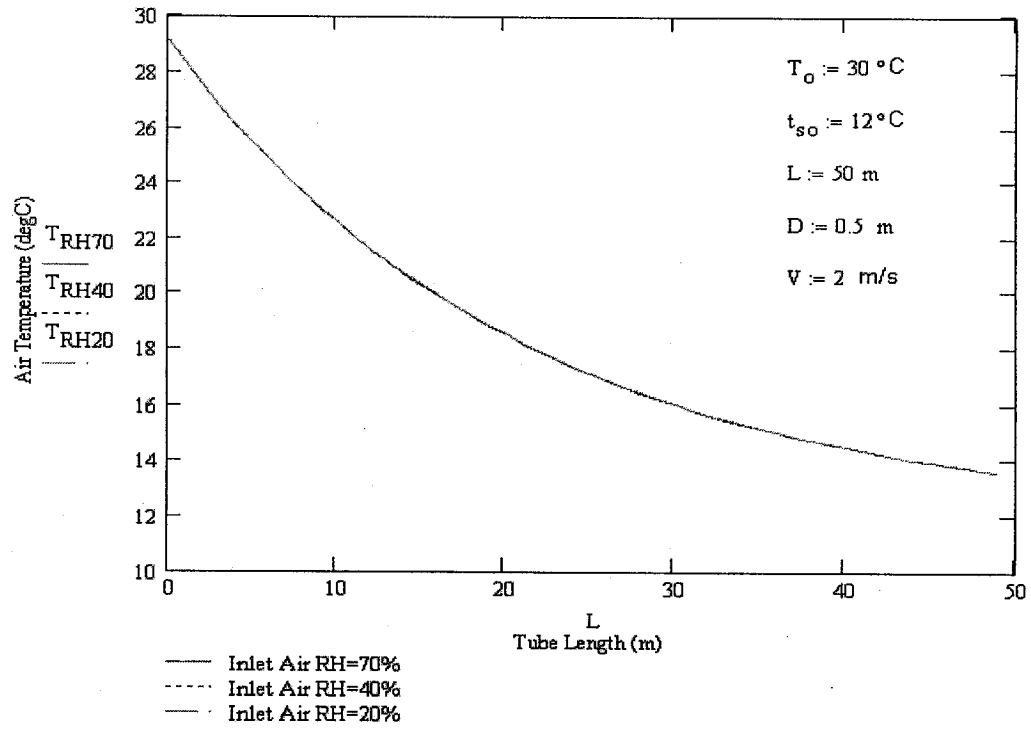
Fig. 4.10 Air temperature inside an ETAHE at different relative humidity
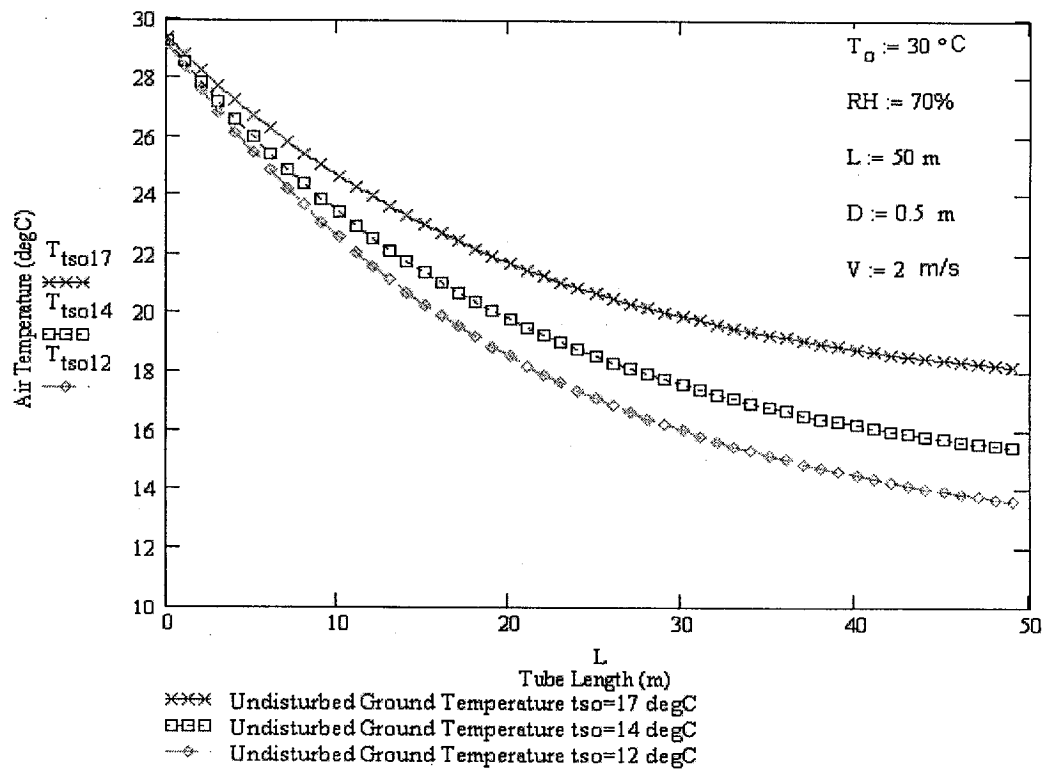

Fig. 4.11 Air temperature inside an ETAHE at different undisturbed soil temperature

57
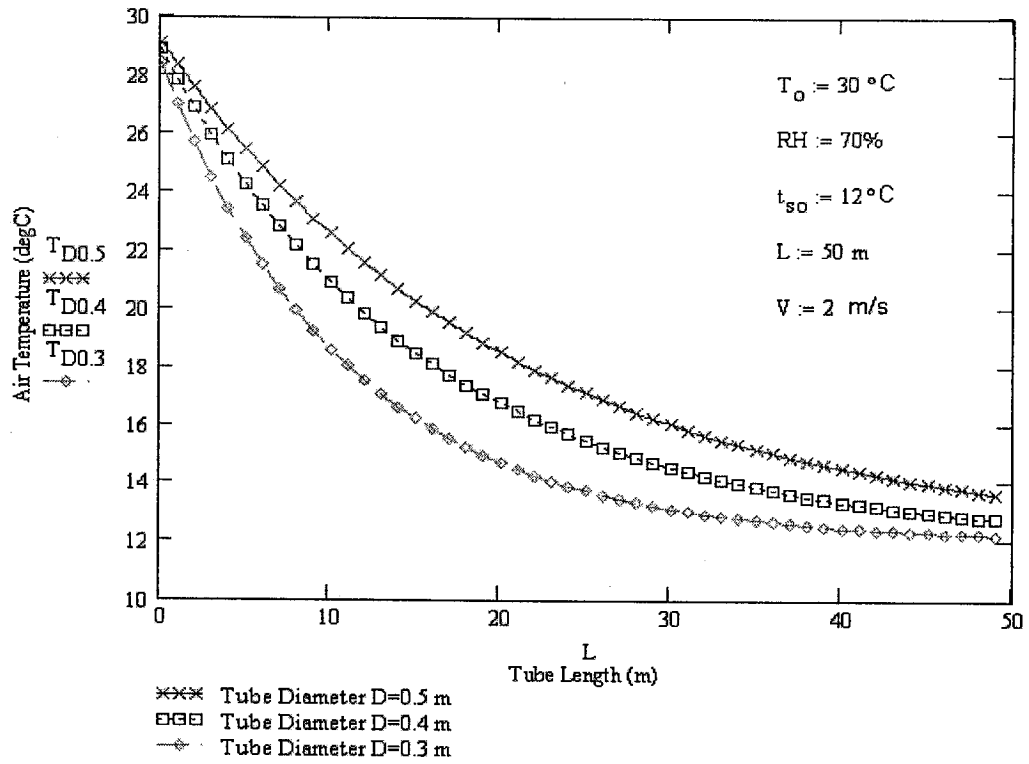
Fig. 4.12 Air temperature inside an ETAHE at different tube diameter
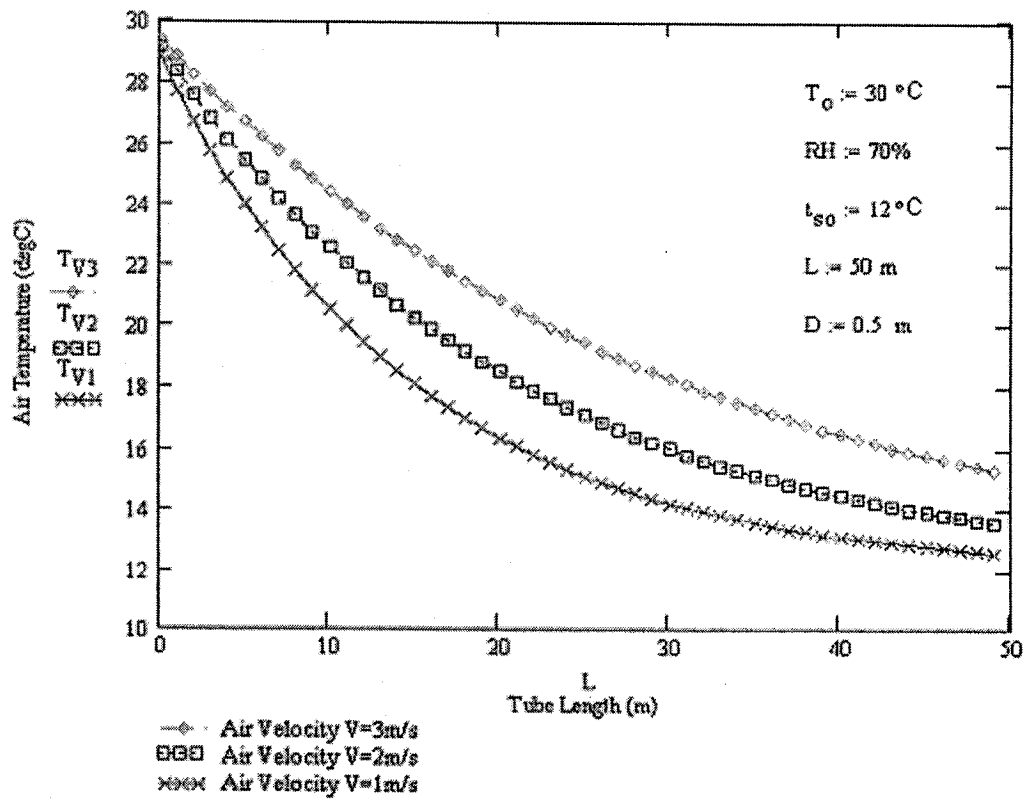
Fig. 4.13 Air temperature inside an ETAHE at different inlet air velocity

4.6 Analysis of Montreal meteorological data and ETAHE applications

Figure 4.14 and Figure 4.15 show published ambient air temperature and water-vapor pressure for a whole year in Montreal. By calculation according to psychometrics theory [ASHRAE Handbook-Fundamentals, 2001], we obtain Montreal hourly air relative humidity (Figure 4.16). In the process of calculation, the undisturbed ground temperature is one of main input parameters. However, its accurate modeling is difficult because the soil parameters are often unknown and there are also no published hourly soil temperature data available.

Figure 4.17 shows only monthly average soil temperatures at different depth and monthly ambient air average temperature in Montreal. Here, we study a 50m long tube with a diameter of 0.5m buried at 3m underground in Montreal. Assuming the air velocity is 2m/s, we run the program to obtain the monthly average outlet air temperature as showed also in Figure 4.17. Results demonstrate that in February the outdoor air can be heated from -10°C to around -1°C and in July be cooled from 21°C to 12°C. Obviously, the cooling and heating potential are huge.

A further 48-hour performance analysis for the same ETAHE, showed in Figure 4.18 for two typical summer days and Figure 4.19 for two typical winter days, indicates that in summer, the daily ambient temperature variation is narrowed from 12°C to 3°C and in winter it is narrowed from 9°C to 2°C. In winter, outlet air temperature from the ETAHE still needs to be reheated before being distributed because it is under freezing point.
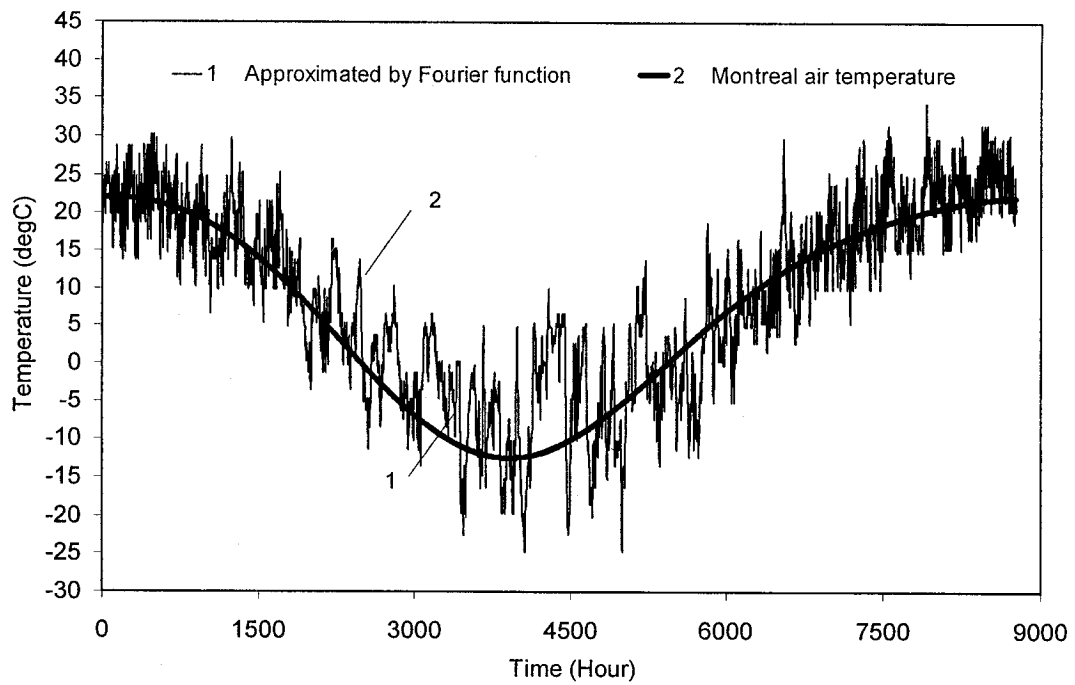
Fig. 4.14 Montreal air temperature (from Atmospheric Environment Service)
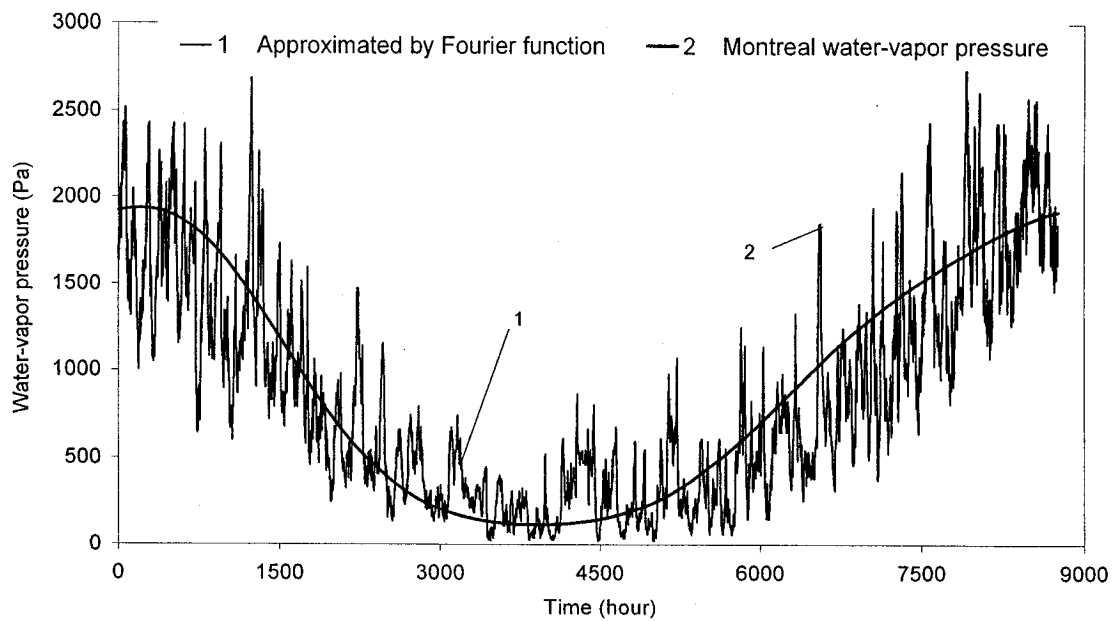
Fig. 4.15 Montreal water-vapor pressure (from Atmospheric Environment Service)
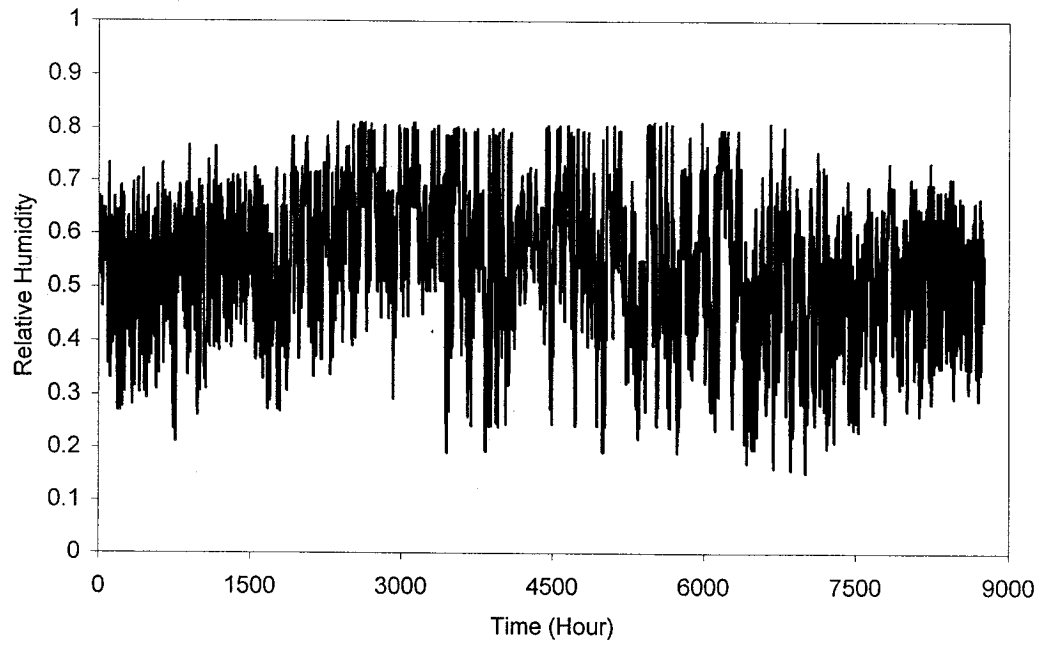
Fig. 4.16 Montreal relative humidity
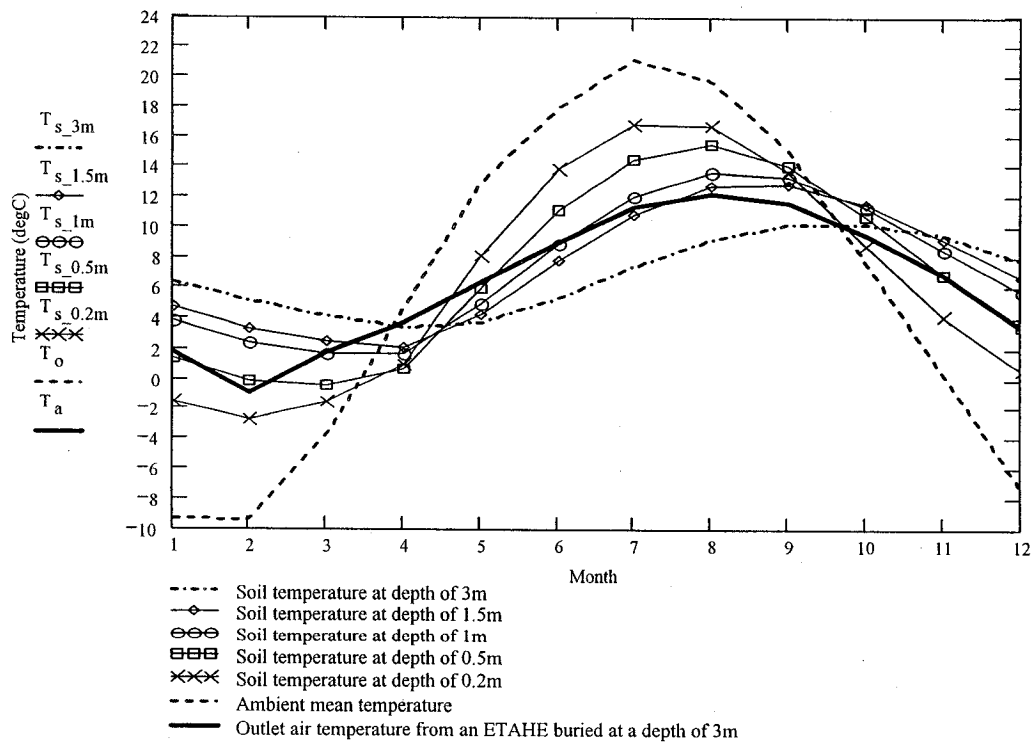
Fig. 4.17 Steady analysis of the yearly performance of an ETAHE in Montreal's climate

61
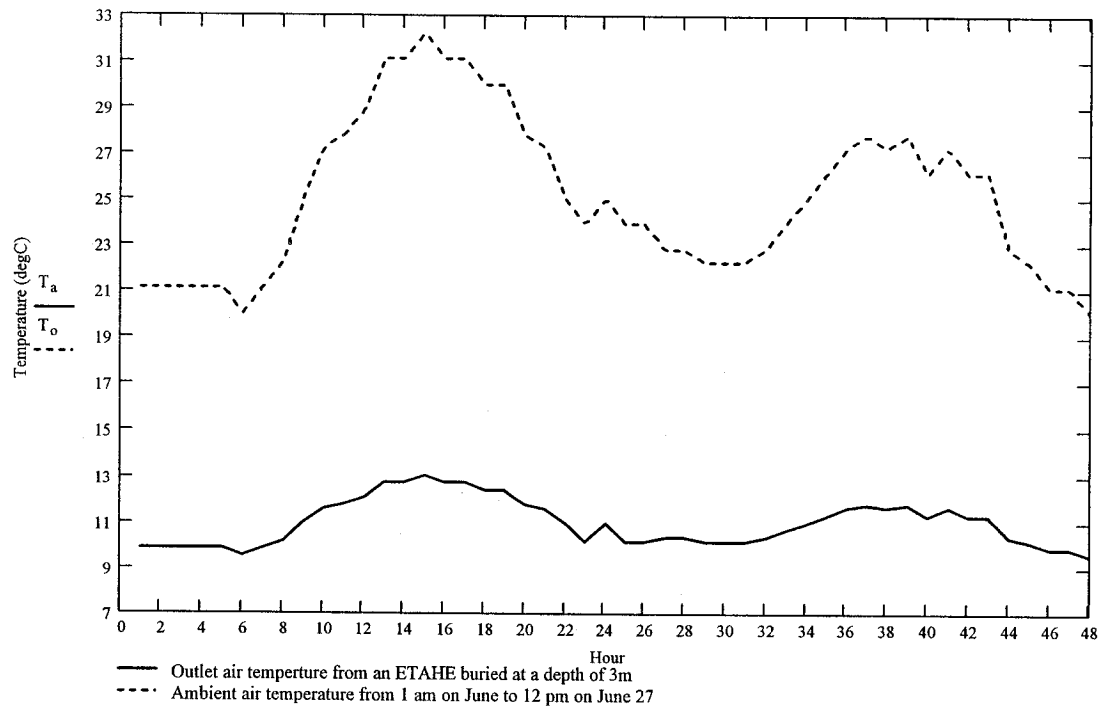
Fig. 4.18 48 hours performance analysis of an ETAHE in Montreal's summer climate
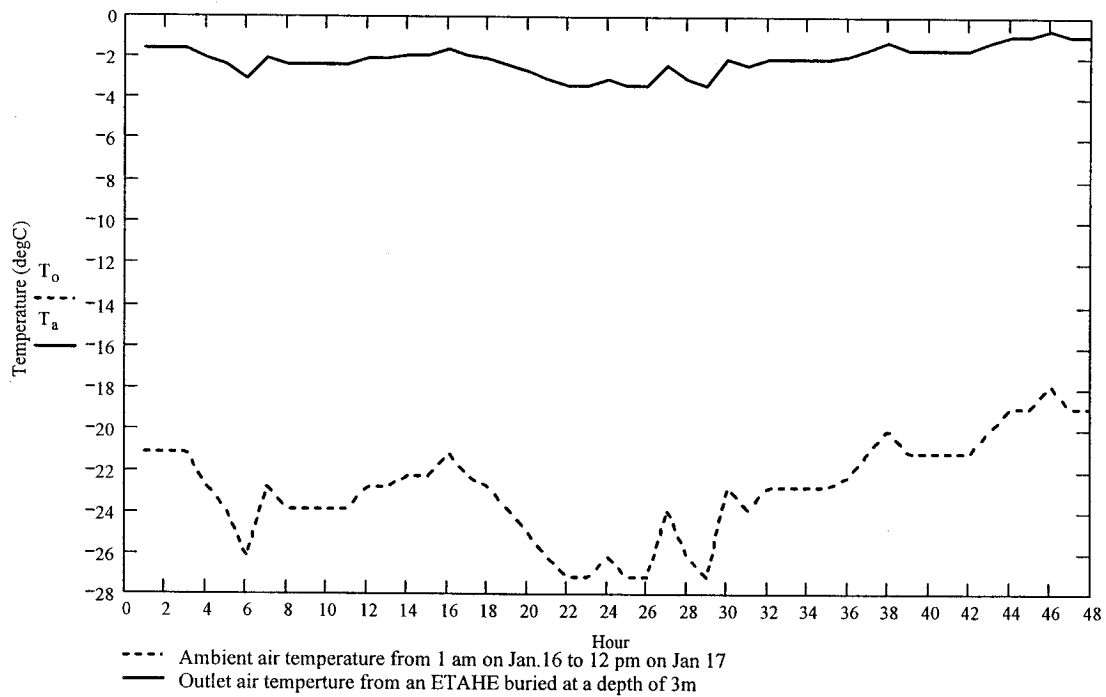
Fig. 4.19 48 hours performance analysis of an ETAHE in Montreal's winter climate

CHAPTER 5

CONCLUSIONS AND RECOMMENDATIONS

5.1 Conclusions

A 1-D transient thermal network model has been developed to determine the soil temperature variation around an ETAHE. It was found that the soil temperature near the tube increases only around 2°C after ten hours' continuous operation.

Based on this finding and guidelines from literature, a reasonable assumption was made for a new 1-D steady-state model, which was developed to investigate the performance of an ETAHE. Unlike a number of other 1-D models, this model can predict not only air temperature, but also relative humidity along the ETAHE by combining an analytical solution and a control volume methodology. Simpler than most multi-dimensional models, which are usually solved by commercial software, the new model may be used by design engineers to size and optimize the ETAHE systems. Moreover, it can determine how much condensation there will be and where it will occur. This is very important for designers to prevent mould from growing in the system.

Simulation results show that the ETAHE system has great potential to meet both heating and cooling loads. However, air relative humidity may either reach an uncomfortably high level in summer or drop to an unpleasant low one in winter. Another drawback of the system is that condensation may occur in the summer. Therefore, this system should be used in combination with a regular air conditioner or a humidification/dehumidification system in summer and a humidifier in winter. An additional finding is that condensation starts from the inlet section, which needs to be

validated in future experiments. Simulation results were validated by two sets of published experimental data indicating that the model is accurate enough in predicting the temperatures along an ETAHE.

A sensitivity analysis has shown that the main parameters determining the air temperature at the outlet of the ETAHE are the inlet air temperature and the undisturbed ground temperature, which is a function of the depth at which the ETAHE is placed. The sensitivity analysis has shown also that after a certain limit of length, changing diameter of the tube or the air velocity in the tube does not significantly alter the outlet air temperature. Before that limit, both a smaller diameter of the tube and a higher air velocity in the tube can improve the performance of the system. It is also found that latent heat transfer has little influence on overall performance of the ETAHE since latent heat flux is too small compared with the sensible one.

A further analysis has been carried out to investigate the potential application in Montreal's climate. Results show:

1. In winter, a typical ETAHE system may preheat the outdoor air around 10°C from December to March, but in severe weather during the period, outlet air temperature may be still under freezing point. So the air has to be reheated again before being distributed.

2. For a typical summer day, a 50m long ETAHE with a diameter of 0.5m may cool outdoor air from 30°C to as low as 20°C. In summer, a typical ETAHE system may precool the outdoor air around 10°C from July to September. This shows the usefulness of this technique for passive cooling.

The theoretical model presented here may be helpful in determining the COP of the system from which an economic analysis can be made. One must be cautioned that it is very important to know the soil thermal properties and the undisturbed ground temperature at the location where this method is considered.

It should be stressed that knowledge of accurate values of the convective heat and mass transfer coefficients is important for simulation.

5.2 Future work

This model is still in its first stage of development, but already it is a valuable tool to assist the design and calculation of ETAHE systems forming parts of air-conditioning system of buildings. For different layouts of the ETAHE and air flow rate, resulting temperatures and relative humidity can be calculated. However, there are many works left to do.

One of the short-term goals is to develop a windows-based program independent of MathCAD. A refined version of the program will allow the input of more detailed ground coverings and structures above the ETAHE. A better coupling with building simulation programs raises the possibility to use real weather profiles and hence make the calculation of air properties more accurate. It would also be useful to perform a CFD analysis to compare to the simulation results.

Another recent work is to set up an experiment to investigate where condensation occurs in the tube and how much the condensation flow rate and how it affects the overall performance of the ETAHE.

Even though all of these short-term goals are achieved, there is still a lot of work to be done in the long run. First of all, data on ETAHE operation are limited, and there is a need for data on long-term, time-dependent operation of an ETAHE system to draw conclusions on the long-term system performance. Economic feasibility of the technique must be also considered by comparing it with other conventional air-conditioning technique. Better comparison is expected when time-dependent experimental data are available. The recent project of the Cité du Cirque with ETAHEs in Montreal provides us a useful opportunity for gathering necessary operational data in order to realize our goals.

Secondly, a detailed implicit transient 3-D model needs to be developed. Theoretically, this model should simulate the system more accurately by applying more realistic assumptions so that a time-dependent temperature and moisture profiles both for ground and for air are able to be found. They are important because they would become the tool for finding the daily and yearly control schemes for the system. How to integrate an ETAHE system with a building and how to control it are also two questions to answer.

REFERENCES

1. Abrams D. W., "Low-energy Cooling: A Guide to the Practical Application of Passive Cooling and Cooling Energy Conservation Measures", Van Nostrand Reinhold Company Inc., 1986.

2. Arzano L. and Goswami D. Y., "Performance analysis of a closed loop underground air tunnel for residential housing in a hot and humid climate", http://wire0.ises.org/wire/doclibs/KoreaConf.nsf/id/41FEAAA2836D4B47C1256 5A0004F3E49/$File/7-649-1.PDF.

3. ASHRAE Handbook-Fundamentals, Ch. 5 and Ch. 6, Atlanta, Georgia, 2001.

4. ASHRAE Handbook-HVAC systems and equipments, Ch.11, Atlanta, Georgia, 2000.

5. Athienitis K. A., "Building Thermal Analysis", Ch.8, Electronic handbook, 3rd edition, 1998.

6. Athienitis K. A., and Santamouris M., "Thermal analysis and design of passive solar buildings", James & James Pub., London, UK, 2002.

7. Bansal N. K. and Sod M. S., "An earth-air tunnel system for cooling buildings", Tunnelling and Underground Space Technology, Volume 1, Issue 2, pp. 177-182, 1986.

8. Benkert S., Heidt F. D. and Scholer D., "Calculation tool for earth heat exchangers GAEA", http://www.hvac.okstate.edu/pdfs/bs97/papers/P008.PDF

9. Benkert S. and Heidt F. D., "Designing earth heat exchangers with GAEA", EuroSun, IV.2.2-1, 1998.

10. Bojic M., Trifunovic N., Papadakis G., and Kyritsis S., "Numerical simulation, technical and economic evaluation of air-to-earth heat exchanger coupled to a building, Energy, Vol. 22, pp. 1151-1158, 1997.

11. Bojic M., Papadakis G. and Kyritsis S., "Energy from a two-pipe, earth-to-air heat exchanger", Energy Vol. 24, pp. 519-523, 1999.

12. Boulard T., Razafinjohany E. and Baille A., "Heat and water vapour transfer in a greenhouse with an underground heat storage system part I. Experimental results", Agricultural and Forest Meteorology, Volume 45, Issues 3-4, pp. 175-184, March 1989.

13. Bourret B. and Soontornchainachsaeng T., "Model of the behaviour of an earth tube heat exchanger: simplified analytical approach and validation" (in French), Entropie, Vol. 30, No. 181, pp. 35-41, 1994.

14. Bowman W. J. Bishop P. J., "Examination of the feasibility of an earth coolant tube to provide residential space cooling", ASHRAE Transactions, No. 3053, pp. 626-640, 1987.

15. Carmody J.C., Meixel G. D., Labs K. B. and Shen L. S., "Earth-contact buildings Applications, Thermal analysis and energy benefits", Advances in Solar Energy, Vol. 2, Chapter 6, pp. 297-347, 1985.

16. Correia da Silva J.J., Silva A. M. and Fernandes E. O., "Passive cooling in livestock buildings", Seventh International IBPSA Conference, 2001.

17. De Paepe M., Mlecnik E., De Bruyn G., Govers K., Van Dyck T., Bossaer A. and Baert K., "Earth-air heat exchangers in the Belgian climate: first practical experience", 22nd Annual AIVC Conference, Bath, UK, 11-14 September 2001.

18. De Paepe M., "Earth-air heat exchangers in the Belgian climate: Analysis of the potential with a 3D modeling technique", 22nd Annual AIVC Conference, Bath, UK, 11-14 September 2001.

19. De Paepe M. and Janssens A., "Thermo-hydraulic design of earth-air heat exchangers", Energy and Buildings, Vol. 35, No. 4, pp. 389-397, May 2003.

20. Dhia A., "Earth-tube heat exchangers for poultry buildings", Agricultural Mechanization in Asia, Africa and Latin America, Vol. 26, No. 4, pp. 62-64, 1995.

21. EREC Reference Briefs, "Earth Cooling Tubes", U.S. Department of Energy, 2002.

22. Gauthier C., Lacroix M. and Bernier H., "Numerical simulation of soil heat exchanger-storage systems for greenhouses", Solar Energy, Vol. 60, pp. 333-346, 1997.

23. Gieseler U. D. J., Bier W. and Heidt F. D., "Cost efficiency of ventilation systems for low-energy buildings with earth-to-air heat exchange and heat recovery", Proceedings of the Intern. Conference on Passive and Low Energy Architecture (PLEA), Toulouse, 2002.

24. Givoni B., "Passive and low energy cooling of buildings", Van Nostrand Reinhold Company Inc., 1994.

25. Goswami D. Y. and Dhaliwal A. S., "Heat transfer analysis in environmental control using an underground air tunnel", Journal of Solar Energy Engineering, Vol. 107, pp. 141-145, 1985.

26. Goswami D. Y. and Ileslamlou S., "Performance analysis of a closed-loop climate control system using underground air tunnel", Journal of Solar Energy Engineering, Vol. 112, pp.76-81, May 1990.

27. Gustafsson S-I., "Are earth tube exchangers of interest when heating buildings?", Interational Journal of Energy Research, Vol. 17, No. 7, pp. 597-604, 1993.

28. Hokkanen V., Forssén I., Niva M., Sorjonen K. and Lahti Institute of Design, "Four examples of subsurface uses in Finland", Tunnelling and Underground Space Technology, Volume 9, Issue 3, pp. 385-393, July 1994.

29. Hollmuller P., "Analytical characterisation of amplitude-dampening and phase-shifting in air/soil heat-exchangers", International Journal of Heat and Mass Transfer, Volume 46, Issue 22, pp. 4303-4317, October 2003a.

30. Hollmuller P. and Lachal B., "Cooling and preheating with buried pipe systems: monitoring, simulation and economic aspects", Energy and Building, 2003b.

31. Holman J. P., "Heat Transfer", McGraw-Hill, ninth edition, 2002

32. IEA Annex 28, Early design guidance for low energy cooling technologies, International Energy Agency, Energy Conservation in Buildings and Community Systems Program, Annex 28 Low Energy Cooling, Subtask 2, Report 2, 1999.

33. Kaushik S. C. and Kumar G. S., "Performance evaluation of an earth air tunnel for space heating of a non air-conditioned building", International Journal of Ambient Energy, Vol. 15, No. 4, pp. 205-218, October 1994.

34. Kumar R., Ramesh S. and Kaushik S. C., "Performance evaluation and energy conservation potential of earth-air-tunnel system coupled with non-air-conditioned building", Building and Environment, Vol. 38, pp. 807-813, 2003.

35. Labs K., "Earth Coupling", Solar Heat Technologies: Fundamentals and Applications, Chapter 5, pp.197-346, The MIT Press, 1989.

36. Lemay S. P., Marquis A. and D'allaire S., "Environmental conditions in a growing-finishing swine building ventilated with and without earth tube heat exchanger", Canadian Agricultural Engineering, Vol. 36, No. 4, pp. 263-271, 1994.

37. Lemay S. –P. and Marquis A., "Performance of earth tube heat exchangers in a growing-finishing swine building", Applied Engineering in Agriculture, Vol. 11, No. 6, pp. 887-895, 1995.

38. Levit H. J., Gaspar R. and R. D. Piacentini, "Simulation of greenhouse microclimate produced by earth tube heat exchangers", Agricultural and Forest Meteorology, Volume 47, Issue 1, pp. 31-47, July 1989.

39. Mavroyanopoulos G. N. and Kyritsis S., "The performance of a greenhouse heated by an earth-air heat exchanger", Agricultural and Forest Meteorology, Volume 36, Issue 3, pp. 263-268, February 1986.

40. Meliß M. and Späte F., "The solar heating system with seasonal storage at the Solar-Campus Jülich", Solar Energy, Volume 69, Issue 6, pp. 525-533, 2000.

41. Mihalakakou G., Lewis J. O., and Santamouris M., "On the heating potential of buried pipes techniques -- application in Ireland", Energy and Buildings, Volume 24, Issue 1, pp. 19-25, 1996.

42. Mihalakakou G., Lewis J. O., and Santamouris M., "The influence of different ground covers on the heating potential of earth-to-air heat exchangers", Renewable Energy, Volume 7, Issue 1, pp. 33-46, January 1996.

43. Mihalakakou G., Santamouris M., Asimakopoulos D. and Tselepidaki I., "Parametric prediction of the buried pipes cooling potential for passive cooling applications", Solar Energy, Volume 55, Issue 3, pp.163-173, September 1995.

44. Mihalakakou G., Santamouris M., and Asimakopoulos D., "Modelling the thermal performance of earth-to-air heat exchangers", Solar Energy, Vol. 53, No. 3, pp. 301-305, 1994.

45. Mihalakakou G., "On the heating potential of a single buried pipe using deterministic and intelligent techniques", Renewable Energy, Volume 28, Issue 6, pp. 917-927, May 2003

46. Nara Y., Horino H., and Mitsuno T., "Collecting evaporated water by an earth-to-air heat exchanger installled in a greenhouse", ACTA Horticulturae, No. 534, pp.245-254, 2000.

47. Pfafferott J., "Evaluation of earth-to-air heat exchangers with a standardised method to calculate energy efficiency", Energy and Buildings, Volume 35, Issue 10, pp. 971-983, November 2003.

48. Santamouris M., Argiriou, and Vallindras M., "Design and operation of low energy consumption passive solar agricultural greenhouse", Solar Energy, Vol. 52, 1994.

49. Santamouris M. and Asimakopolous D., "Passive Cooling of Buildings", James & James Ltd., London, 1996.

50. Santamouris M., Mihalakakou G., Argiriou A. and Asimakopoulos D. N., "On the performance of buildings coupled with earth to air heat exchangers", Solar Energy, Volume 54, Issue 6, pp. 375-380, June 1995.

51. Santamouris M., Mihalakakou G., Balaras C. A., Argiriou A., Asimakopoulos D. and Vallindras M., "Use of buried pipes for energy conservation in cooling of agricultural greenhouses", Solar Energy, Volume 55, Issue 2, pp. 111-124, August 1995.

52. Shingari B. K., Singh A., and Sapra K. L., "Earth tube heat exchangers", Poultry International, V. 34, No. 14, pp. 92-96, 1995.

53. Singh A. K., Tiwari G. N., Lugani N. and Garg H. P., "Energy conservation in a cinema hall under hot and dry condition", Energy Conversion and Management, Volume 37, Issue 5, pp. 531-539, May 1996.

54. Sodha M. S., Sharma A. K., Singh S. P., Bansal N. K., and Kumar A., "Evaluation of an earth-air-tunnel system for cooling/heating of a hospital complex", Building and Environment, Vol. 20(2), pp.115-22, 1985.

55. Sutar R. F. and Tiwari G. N., "Temperature reductions inside a greenhouse", Fuel and Energy Abstracts, Volume 37, Issue 2, pp.133, March 1996

56. Tiwari G. N., Sutar R. F., Singh H. N. and Goyal R. K., "Performance studies of earth air tunnel cum greenhouse technology", Energy Conversion and Management, Volume 39, Issue 14, 15, pp. 1497-1502, September 1998.

57. Trombe A. and Serres L., "Air-earth exchanger study in real site experimentation and simulation", Energy and Buildings, Volume 21, Issue 2, pp. 155-162, 1994.

58. Tzaferis A., Liparakis D., Santamouris M., and Argiriou A., "Analysis of the accuracy and sensitivity of eight models to predict the performance of earth-to-air heat exchangers", Energy and Buildings, Vol. 18, pp. 35-43, 1992.

59. Wagner R., Beisel S., Spieler A., Vajen K., and Gerber A., "Measurement, modeling and simulation of an earth-to-air heat exchanger in Marburg (Germany)", 4. ISES Europe Solar Congress, Copenhagen, Denmark, 2000.

APPENDIX A:

SEMI-INFINITE SLAB MODELLING

Semi-Infinite Slab: Convective Boundary Condition

A thick floor slab is initially at a uniform temperature Ti. Suddenly, one of its surfaces is subjected to convective cooling with a heat transfer coefficient h into an environment at Te. Calculate the temperature at a depth x from the surface at time t after the change.

Ground may be considered as a semi-infinite slab. This model can be used to determine soil temperature variation due to ambient temperature change. A rectangular ETAHE with a high width to height ratio may be approximately simulated with this model.

$degC \equiv 1$

Properties of floor slab:

$k_s := 1.2 \cdot \dfrac{watt}{m \cdot degC}$ ... Soil thermal conductivity $\rho_s := 1500 \cdot \dfrac{kg}{m^3}$ ... Soil density

$c_s := 1000 \cdot \dfrac{joule}{kg \cdot degC}$ ... Soil specific heat capacity

$\alpha := \dfrac{k_s}{\rho_s \cdot c_s}$ ... Soil thermal diffusivity $\alpha = 8 \times 10^{-7} \dfrac{m^2}{s}$

$h_c := 5 \cdot \dfrac{watt}{m^2 \cdot degC}$ ... Film coefficient at surface

$T_a := 25 \cdot degC$ ... Sol-air temperature

$Ti := 12 \cdot degC$ ... Initial soil-air interface
                                     temperature

$i := 1 .. 80 \quad t_i := i \cdot \dfrac{1.0 \cdot hr}{4} \quad j := 0, 1 .. 10 \quad x_j := j \cdot 0.2 \cdot m$

The temperature at depth x and time t for a semi-infinite slab with convective boundary condition is given by

$$T_{i,j} := (T_a - Ti) \cdot \left[1 - erf\left(\frac{x_j}{2 \cdot \sqrt{\alpha \cdot t_i}} \right) - exp\left(\frac{h_c \cdot x_j}{k_s} + \frac{h_c^2 \cdot \alpha \cdot t_i}{k_s^2} \right) \cdot \left(1 - erf\left(\frac{x_j}{2 \cdot \sqrt{\alpha \cdot t_i}} + \frac{h_c \cdot \sqrt{\alpha \cdot t_i}}{k_s} \right) \right) \right] + Ti$$

$$\frac{T_{i,0}}{}$$

$$\frac{T_{i,1}}{degC}$$

$$\frac{T_{i,10}}{degC}$$

$\frac{t_i}{hr}$

——— T(0m,t)
- - - - T(0.3m, t)
— · — T(2m, t)
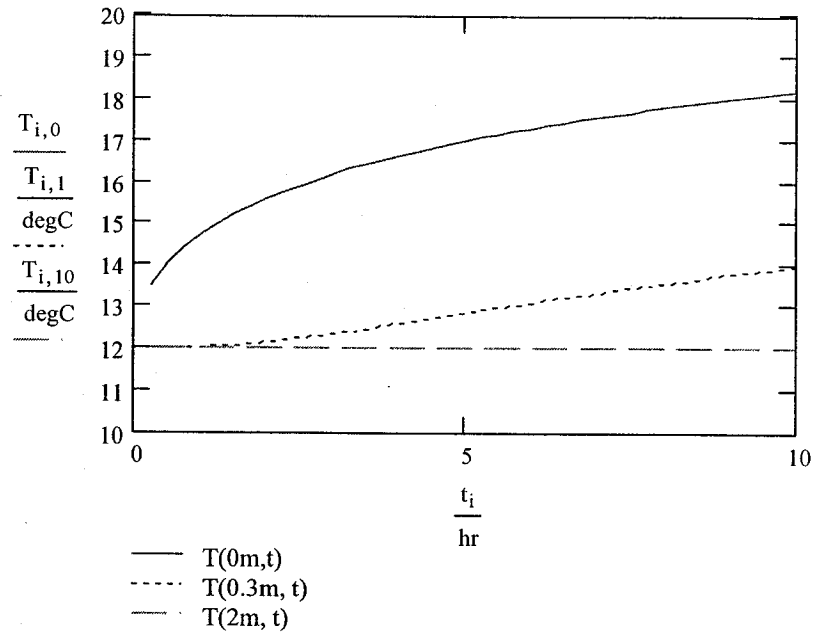
Heat flow at surface at time t:

$$qs_i := h_c \cdot (T_a - Ti) \cdot exp\left(\frac{h_c^2 \cdot \alpha \cdot t_i}{k_s^2} \right) \cdot \left(1 - erf\left(\frac{h_c \cdot \sqrt{\alpha \cdot t_i}}{k_s} \right) \right)$$

$$\frac{qs_i}{watt}$$

$\frac{t_i}{hr}$

79
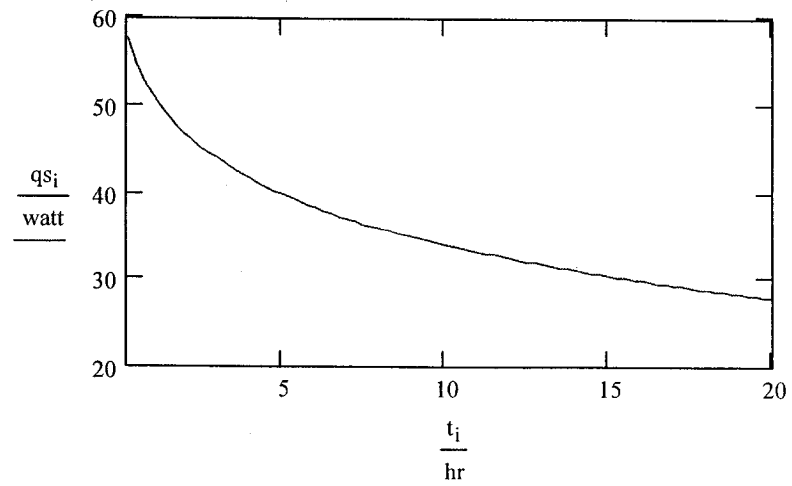
APPENDIX B:

CONTROL VOLUME TRANSIENT 1-D MODEL

Analysis of Heat Conduction in Soil Around an Earth-to-Air Heat Exchanger (ETAHE):

$degC \equiv 1$

$r_{ir} := 0.5 \cdot m$ ... Tube interior radium $r_{or} := 0.55 \cdot m$ ... Tube outer radium

$\Delta c := 0.01 \cdot m$ ... Increment of each nodes $L := 1 \cdot m$ ... Tube length

$k_s := 1.2 \cdot \dfrac{watt}{m \cdot degC}$ ... Soil thermal conductivity $\rho_s := 1800 \cdot \dfrac{kg}{m^3}$ ... Soil density

$c_s := 1300 \cdot \dfrac{joule}{kg \cdot degC}$ ... Soil specific heat capacity

$k_t := 1.7 \cdot \dfrac{watt}{m \cdot degC}$ ... Concrete tube thermal conductivity $\rho_t := 2200 \cdot \dfrac{kg}{m^3}$ ... Concrete tube density

$c_t := 800 \cdot \dfrac{joule}{kg \cdot degC}$ ... Concrete tube specific heat capacity

$i := 0, 1 .. 101$ $j := 1 .. 101$ ... Node index

$r_i := \left(r_{ir} + \Delta c \cdot i^{1.4} \right)$ ... Node radii $r_{101} = 6.898\,m$
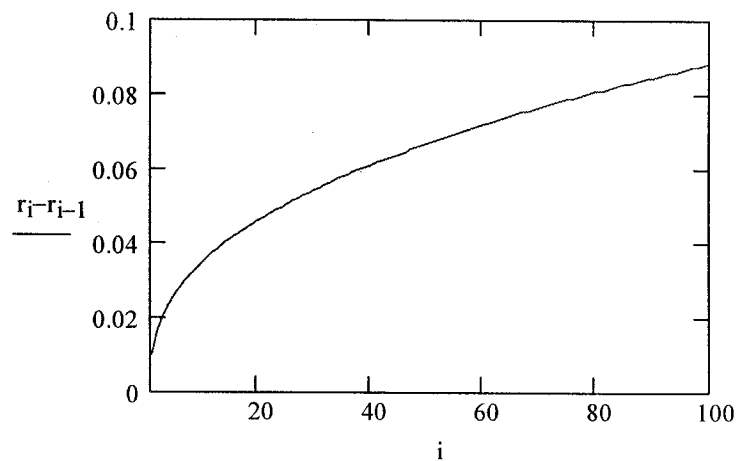
Control volume size at differerent nodes

81

$$h_c := 5 \cdot \frac{watt}{m^2 \cdot degC}$$ . . . convective heat transfer coefficient at tube interior surface

$$Ri := \frac{1}{2 \cdot \pi \cdot r_{ir} \cdot h_c \cdot L}$$ . . . Tube interior film resistance

$$R_j := \frac{\ln\left(\dfrac{r_j}{r_{j-1}}\right)}{2 \cdot \pi \cdot k_s \cdot L}$$ . . . Control volume resistances

$$R_0 := \frac{\ln\left(\dfrac{r_{or}}{r_{ir}}\right)}{2 \cdot \pi \cdot k_t \cdot L}$$ . . . Concrete tube resistance

$$C_j := \pi \cdot L \cdot \left[\left(r_j\right)^2 - \left(r_{j-1}\right)^2 \right] \cdot \rho_s \cdot c_s$$ . . . Control volume capacities

$$C_1 := \pi \cdot L \cdot \left[\left(r_{or}\right)^2 - \left(r_{ir}\right)^2 \right] \cdot \rho_t \cdot c_t$$ . . . Concrete tube capacity

$$N := 8640$$
$$u_j := R_j \cdot C_j$$

$$t := 0, 1 .. N$$ . . .Time index
$$u_1 = 648.041 \, s$$

$$T_a := 25 \cdot degC$$ . . . Air temperature

$$T_s := 12 \cdot degC$$ . . . Undisturbed ground temperature

$$T_{0,j} := T_s$$ . . . Initial condition

Stability test:

$$
TS := \begin{bmatrix}
\dfrac{C_1}{\dfrac{1}{\left(\dfrac{R_1}{2} + R_0 + R_i\right)} + \dfrac{1}{\left(\dfrac{R_1}{2} + \dfrac{R_2}{2}\right)}} & \dfrac{C_2}{\dfrac{1}{\dfrac{R_3+R_2}{2}} + \dfrac{1}{\dfrac{R_1+R_2}{2}}} \\[4em]
\dfrac{C_3}{\dfrac{1}{\dfrac{R_3+R_4}{2}} + \dfrac{1}{\dfrac{R_3+R_2}{2}}} & \dfrac{C_4}{\dfrac{1}{\dfrac{R_5+R_4}{2}} + \dfrac{1}{\dfrac{R_4+R_3}{2}}} \\[4em]
\dfrac{C_5}{\dfrac{1}{\dfrac{R_6+R_5}{2}} + \dfrac{1}{\dfrac{R_4+R_5}{2}}} & \dfrac{C_6}{\dfrac{1}{\dfrac{R_7+R_6}{2}} + \dfrac{1}{\dfrac{R_5+R_6}{2}}} \\[4em]
\dfrac{C_7}{\dfrac{1}{\dfrac{R_7+R_8}{2}} + \dfrac{1}{\dfrac{R_6+R_7}{2}}} & \dfrac{C_8}{\dfrac{1}{\dfrac{R_9+R_8}{2}} + \dfrac{1}{\dfrac{R_7+R_8}{2}}} \\[4em]
\dfrac{C_9}{\dfrac{1}{\dfrac{R_{10}+R_9}{2}} + \dfrac{1}{\dfrac{R_8+R_9}{2}}} & \dfrac{C_{10}}{\dfrac{1}{\left(\dfrac{R_{10}}{2}\cdot1.5\right)} + \dfrac{1}{\left(\dfrac{R_9}{2} + \dfrac{R_{10}}{2}\right)}}
\end{bmatrix}
$$

$$
TS = \begin{pmatrix}
833.478 & 97.746 \\
155.634 & 205.997 \\
252.988 & 297.711 \\
340.723 & 382.366 \\
422.871 & 396.979
\end{pmatrix} s
$$

The time step Dt should be lower than the minimum of the values in the matrix TS

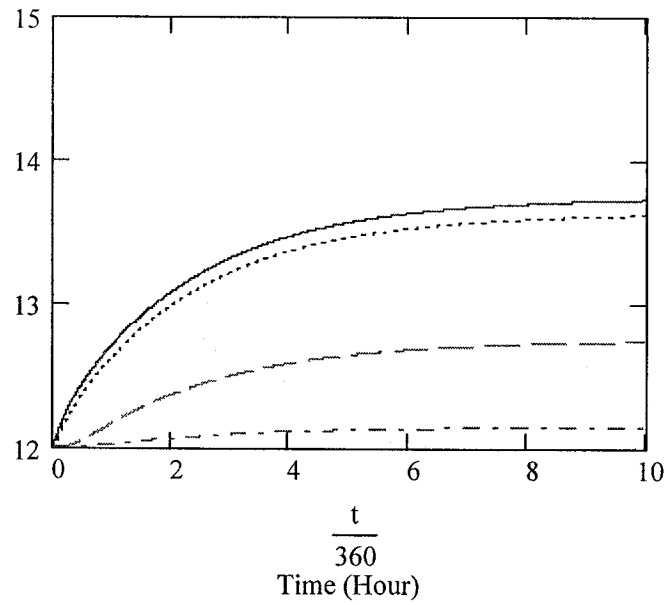$\Delta t_{critical} := \min(TS)$ $\Delta t_{critical} = 97.746\,sec$

$\Delta t := 30\cdot sec$

Ten nodes analysis

In this case, assume soil thickness is $0.751\,\text{m}$ that is $r_{10} = 0.751\,\text{m}$

$$\begin{pmatrix} T_{t+1,1} \\ T_{t+1,2} \\ T_{t+1,3} \\ T_{t+1,4} \\ T_{t+1,5} \\ T_{t+1,6} \\ T_{t+1,7} \\ T_{t+1,8} \\ T_{t+1,9} \\ T_{t+1,10} \end{pmatrix} := \begin{bmatrix} \dfrac{\Delta t}{C_1}\left(\dfrac{T_a - T_{t,1}}{\dfrac{R_1}{2}+R_0+Ri} + \dfrac{T_{t,2}-T_{t,1}}{\dfrac{R_1}{2}+\dfrac{R_2}{2}}\right)+T_{t,1} \\[2em] \dfrac{\Delta t}{C_2}\left(\dfrac{T_{t,3}-T_{t,2}}{\dfrac{R_3+R_2}{2}} + \dfrac{T_{t,1}-T_{t,2}}{\dfrac{R_1+R_2}{2}}\right)+T_{t,2} \\[2em] \dfrac{\Delta t}{C_3}\left(\dfrac{T_{t,4}-T_{t,3}}{\dfrac{R_3+R_4}{2}} + \dfrac{T_{t,2}-T_{t,3}}{\dfrac{R_3+R_2}{2}}\right)+T_{t,3} \\[2em] \dfrac{\Delta t}{C_4}\left(\dfrac{T_{t,5}-T_{t,4}}{\dfrac{R_5+R_4}{2}} + \dfrac{T_{t,3}-T_{t,4}}{\dfrac{R_4+R_3}{2}}\right)+T_{t,4} \\[2em] \dfrac{\Delta t}{C_5}\left(\dfrac{T_{t,6}-T_{t,5}}{\dfrac{R_6+R_5}{2}} + \dfrac{T_{t,4}-T_{t,5}}{\dfrac{R_4+R_5}{2}}\right)+T_{t,5} \\[2em] \dfrac{\Delta t}{C_6}\left(\dfrac{T_{t,7}-T_{t,6}}{\dfrac{R_7+R_6}{2}} + \dfrac{T_{t,5}-T_{t,6}}{\dfrac{R_5+R_6}{2}}\right)+T_{t,6} \\[2em] \dfrac{\Delta t}{C_7}\left(\dfrac{T_{t,8}-T_{t,7}}{\dfrac{R_7+R_8}{2}} + \dfrac{T_{t,6}-T_{t,7}}{\dfrac{R_6+R_7}{2}}\right)+T_{t,7} \\[2em] \dfrac{\Delta t}{C_8}\left(\dfrac{T_{t,9}-T_{t,8}}{\dfrac{R_9+R_8}{2}} + \dfrac{T_{t,7}-T_{t,8}}{\dfrac{R_7+R_8}{2}}\right)+T_{t,8} \\[2em] \dfrac{\Delta t}{C_9}\left(\dfrac{T_{t,10}-T_{t,9}}{\dfrac{R_{10}+R_9}{2}} + \dfrac{T_{t,8}-T_{t,9}}{\dfrac{R_8+R_9}{2}}\right)+T_{t,9} \\[2em] \dfrac{\Delta t}{C_{10}}\left(\dfrac{T_s - T_{t,10}}{\dfrac{R_{10}}{2}\cdot 1.5} + \dfrac{T_{t,9}-T_{t,10}}{\dfrac{R_9}{2}+\dfrac{R_{10}}{2}}\right)+T_{t,10} \end{bmatrix}$$

$$r_1 = 0.51\,\text{m}$$

$$r_2 = 0.526\,\text{m}$$

$$r_7 = 0.652\,\text{m}$$

$$r_{10} = 0.751\,\text{m}$$

$T_{t,1}$ ———

$T_{t,2}$ - - - - -

$T_{t,7}$ — — —

$T_{t,10}$ — · — ·

$\dfrac{t}{360}$

Time (Hour)

$$q_t := \frac{T_a - T_{t,1}}{\dfrac{R_1}{2} + R_0}$$

$\dfrac{q_t}{W}$
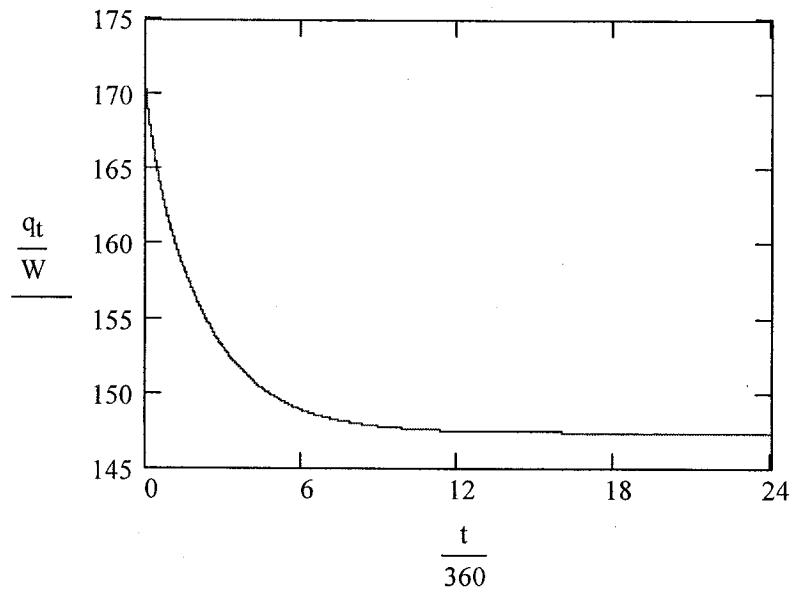
$\dfrac{t}{360}$

85

One hundred nodes analysis

In this case, assume soil thickness is $6.81\,m$ that is $r_{100} = 6.81\,m$

$$
\begin{pmatrix} T_{t+1,1} \\ T_{t+1,2} \\ T_{t+1,3} \\ T_{t+1,4} \\ T_{t+1,5} \\ \blacksquare \\ \blacksquare \\ \blacksquare \\ T_{t+1,99} \\ T_{t+1,100} \end{pmatrix} :=
\begin{bmatrix}
\dfrac{\Delta t}{C_1} \cdot \left(\dfrac{Tf - T_{t,1}}{\dfrac{R_1}{2} + R_0 + Ri} + \dfrac{T_{t,2} - T_{t,1}}{\dfrac{R_1}{2} + \dfrac{R_2}{2}} \right) + T_{t,1} \\[3em]
\dfrac{\Delta t}{C_2} \cdot \left(\dfrac{T_{t,3} - T_{t,2}}{\dfrac{R_3 + R_2}{2}} + \dfrac{T_{t,1} - T_{t,2}}{\dfrac{R_1 + R_2}{2}} \right) + T_{t,2} \\[3em]
\dfrac{\Delta t}{C_3} \cdot \left(\dfrac{T_{t,4} - T_{t,3}}{\dfrac{R_3 + R_4}{2}} + \dfrac{T_{t,2} - T_{t,3}}{\dfrac{R_3 + R_2}{2}} \right) + T_{t,3} \\[3em]
\dfrac{\Delta t}{C_4} \cdot \left(\dfrac{T_{t,5} - T_{t,4}}{\dfrac{R_5 + R_4}{2}} + \dfrac{T_{t,3} - T_{t,4}}{\dfrac{R_4 + R_3}{2}} \right) + T_{t,4} \\[3em]
\dfrac{\Delta t}{C_5} \cdot \left(\dfrac{T_{t,6} - T_{t,5}}{\dfrac{R_6 + R_5}{2}} + \dfrac{T_{t,4} - T_{t,5}}{\dfrac{R_4 + R_5}{2}} \right) + T_{t,5} \\[2em]
\blacksquare \\
\blacksquare \\
\blacksquare \\[2em]
\dfrac{\Delta t}{C_{99}} \cdot \left(\dfrac{T_{t,100} - T_{t,99}}{\dfrac{R_{100} + R_{99}}{2}} + \dfrac{T_{t,98} - T_{t,99}}{\dfrac{R_{98} + R_{99}}{2}} \right) + T_{t,99} \\[3em]
\dfrac{\Delta t}{C_{100}} \cdot \left(\dfrac{T_s - T_{t,100}}{\dfrac{R_{101} + R_{100}}{2}} + \dfrac{T_{t,99} - T_{t,100}}{\dfrac{R_{98} + R_{100}}{2}} \right) + T_{t,100}
\end{bmatrix}
$$

$r_1 = 0.51\,m$

$r_5 = 0.595\,m$

$r_{10} = 0.751\,m$

$r_{20} = 1.163\,m$

$r_{30} = 1.669\,m$

$r_{40} = 2.249\,m$

$r_{100} = 6.81\,m$

$T_{t,1}$

$T_{t,5}$

$T_{t,10}$

$T_{t,20}$

$T_{t,30}$

$T_{t,40}$

$T_{t,100}$

$Tf := 25 \cdot degC$

$Tg := 12 \cdot degC$
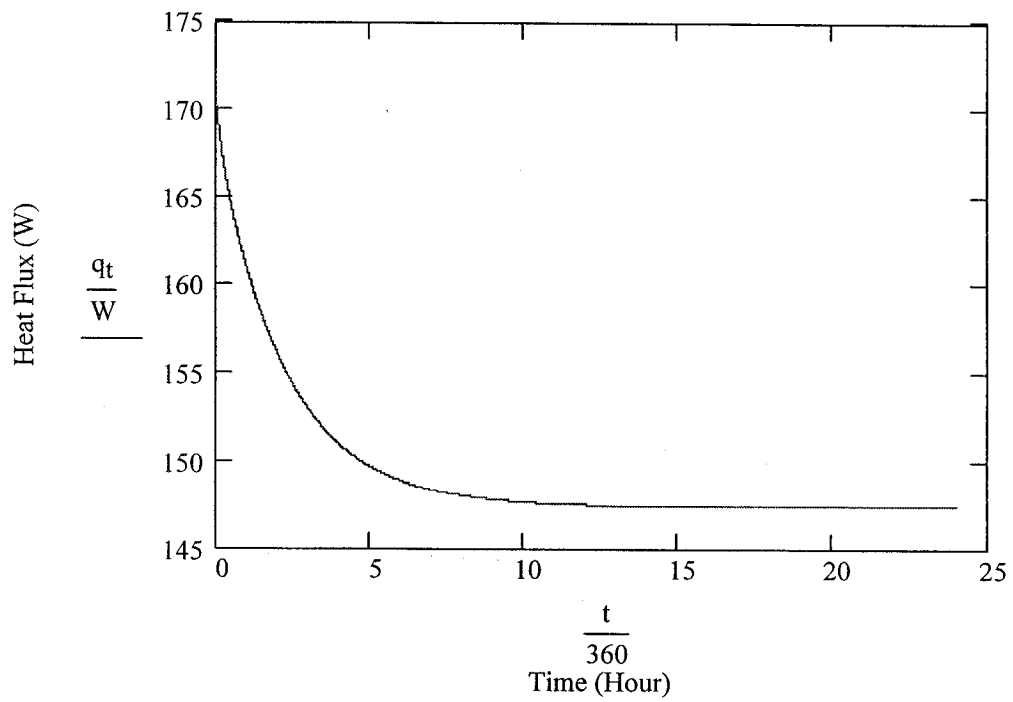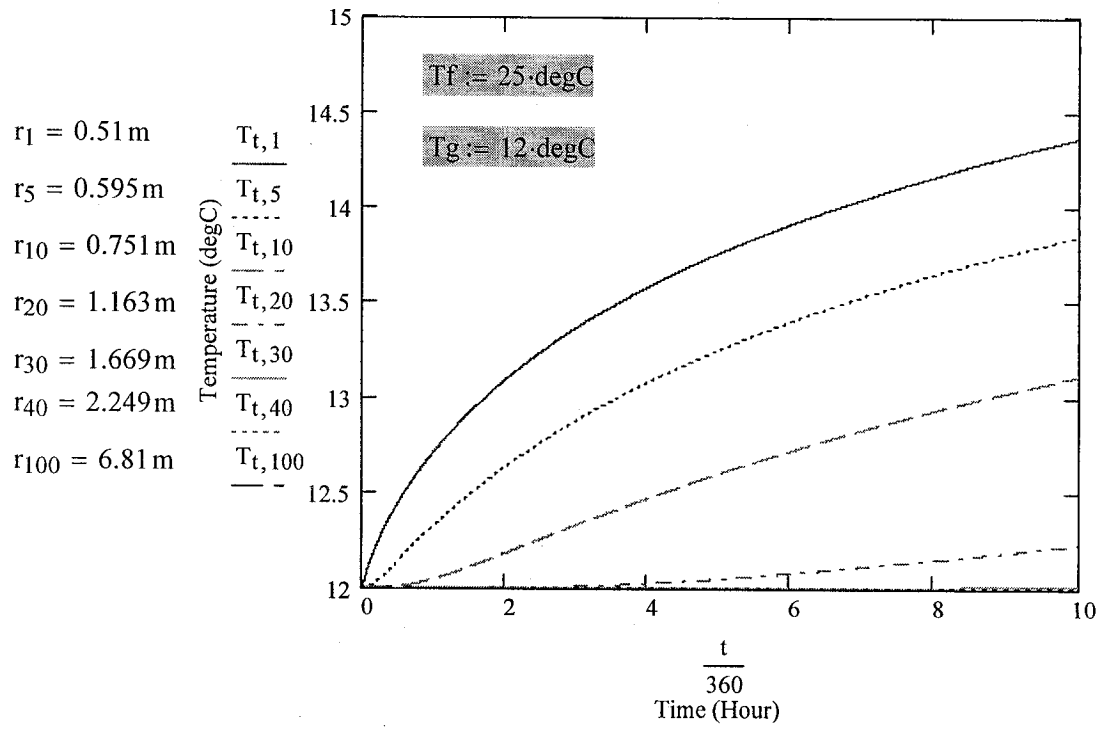
APPENDIX C:

ANALYTICAL MODEL OF ETAHE

(NO CONDENSATION)

CALCULATION OF TEMPERATURE CHANGE OF AIR FLOWING THROUGH AN ETAHE USING ANALYTICAL SOLUTION

Assumptions: 1.No significant change of air temperature occurs while air is flowing through vertical part of wind tower.

2. Air flow is turbulent and velocity is constant.

3. Tube wall keeps isothermal at Ts during operation

Note: highlighted areas are important inputs and results

INPUT DATA $\qquad$ $degC \equiv 1$

$c := 1000 \cdot \dfrac{joule}{kg \cdot degC}$ ... Specific heat of air $\qquad$ $v := 14.5 \cdot 10^{-6} \cdot \dfrac{m^2}{s}$ ... Viscosity of air

$k := 0.024 \cdot \dfrac{W}{m \cdot degC}$ ... Thermal conductivity of air $\qquad$ $\rho := 1.2 \cdot \dfrac{kg}{m^3}$ ... Density of air

$L := 50$ ... Length of tube (m) $\qquad$ $D := 0.5 \cdot m$ ... Diameter of tube (m)

$V := 2 \dfrac{m}{s}$ ... Air velocity $\qquad$ $Q := \pi \cdot \dfrac{D^2}{4} \cdot V$ ... Air flow rate

$i := 0, 1 .. L$ $\qquad$ $X_i := i \cdot m$ $\qquad$ $Q = 1.414 \times 10^3 \dfrac{m^3}{hr}$

$A := \pi \cdot \dfrac{D^2}{4}$ ... Section area of tube $\qquad$ $P := \pi \cdot D$ ... Perimeter of tube

A HEATING CASE:

$To := -10 \cdot degC$ $\qquad$ Outside (ambient) temperature

$Ts := 12 \cdot degC$ $\qquad$ Tube wall (ground) temperature

Calculation of Nusselt number based on Dittus-Boelter relation for turbulent flow:

$$Pr := 0.7 \qquad Re := V \cdot \frac{D}{\nu} \qquad Re = 6.897 \times 10^4$$

$$Nu := 0.023 \cdot Re^{0.8} \cdot Pr^{0.4} \qquad Nu = 148.14 \quad \text{Dittus-Boelter correlation for turbulent flow in tubes}$$

$$h_c := \left(Nu \cdot \frac{k}{D} \right) \qquad h_c := if\left(h_c > 5 \cdot \frac{watt}{m^2 \cdot degC}, h_c, 5 \cdot \frac{watt}{m^2 \cdot degC} \right) \qquad h_c = 7.111 \frac{watt}{m^2 \cdot degC}$$

Differential equation based on heat balance of differential isothermal tube element:

$$V \cdot A \cdot c \cdot \rho \cdot dT = P \cdot dx \cdot h_c \cdot (Ts - T)$$

Thus letting $\qquad a := \dfrac{V \cdot A \cdot c \cdot \rho}{P \cdot h_c} \qquad a = 42.19 \, m$

$$a \cdot \frac{d}{dx}(T - Ts) + (T - Ts) = 0 \quad \text{(note change of T to T-Tw for homogeneous eqution)}$$

$$fa := 1.2 \qquad \text{heat transfer enhancement factor} \qquad a1 := V \cdot A \cdot \frac{c \cdot \rho}{fa \cdot P \cdot h_c}$$

Solution:

$$T_i := Ts + (To - Ts) \cdot e^{\dfrac{-X_i}{a1}}$$

$$T_{50} = 6.694 \, degC \qquad \text{Outlet air temperature with heat transfer enhancement}$$

$$Tnoenh_i := Ts + (To - Ts) \cdot e^{\dfrac{-X_i}{a}}$$

$$Tnoenh_{50} = 5.274 \, degC \quad \text{Outlet air temperature without heat transfer enhancement}$$

Air temperature (degC)

T_i ——

$Tnoenh_i$ -----

X_i

Distance (m) in tube
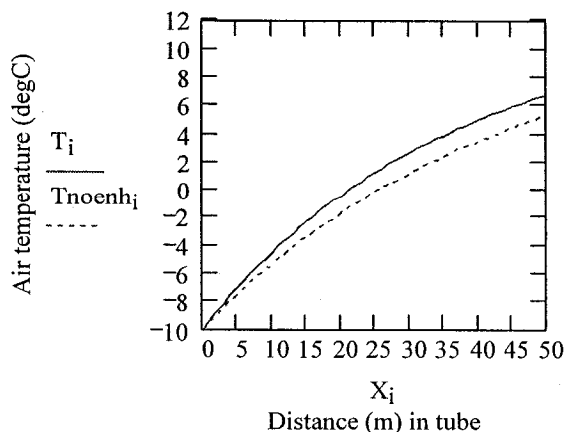
$Ts = 12 \, degC \qquad$ Soil temperature

$To = -10 \, degC \qquad$ Inlet air temperature

$T_{50} = 6.694 \, degC \qquad$ Outlet air temperature

$V = 2 \dfrac{m}{s} \qquad$ Air velocity

90

A COOLING CASE:

$To := 30 \cdot degC$ Outside (ambient) temperature

$Tw := 14 \cdot degC$ Tube wall (ground) temperature

$Nu := 0.023 \cdot Re^{0.8} \cdot Pr^{0.3}$ $Nu = 153.519$

Dittus-Boelter correlation for turbulent flow in ducts

$h_c := \left(Nu \cdot \dfrac{k}{D} \right)$ $h_c := if\left(h_c > 5 \cdot \dfrac{watt}{m^2 \cdot degC}, h_c, 5 \cdot \dfrac{watt}{m^2 \cdot degC} \right)$

$h_c = 7.369 \dfrac{watt}{m^2 \cdot degC}$

Solution:

$T_i := Ts + (To - Ts) \cdot e^{\dfrac{-X_i}{a1}}$ $T_{50} = 16.342$

Outlet air temperature with heat
transfer enhancement

$Tnoenh_i := Ts + (To - Ts) \cdot e^{\dfrac{-X_i}{a}}$ $Tnoenh_{50} = 17.503$

Outlet air temperature without heat
transfer enhancement
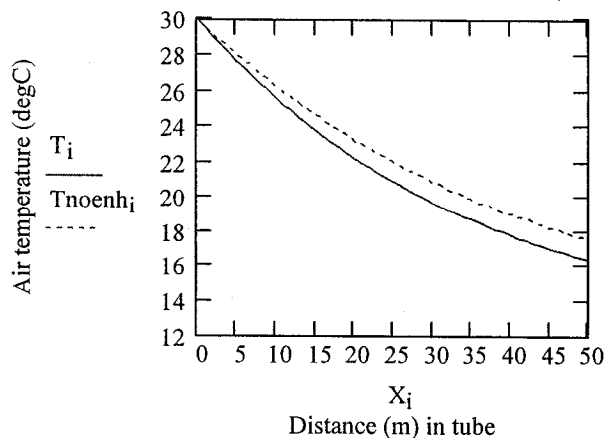
$Tw = 14 \, degC$ Soil temperature

$To = 30 \, degC$ Inlet air temperature

$T_{50} = 16.342 \, degC$

Outlet air temperature

$V = 2 \dfrac{m}{s}$ Air velocity

91

APPENDIX D:

NUMERICAL STEADY-STATE MODEL FOR ETAHE

(WITH CONDENSATION)

DATA INPUT

$t_o := 30$ ... Inlet air temperature (° C) $RH_o := 0.7$ ... Inlet air relative humidity

$t_{so} := 14$ ... Undisturbed ground temperature (° C)

$D := 0.5$ ... Duct diameter (m) $L := 50$ ... Duct length (m)

$N := 50$ ... Control volume number $V := 2$ ... Air velocity (m/s)

Air Properties:

$c := 1000$ ... Specific heat of air (J/kg.K) $v := 14.5 \cdot 10^{-6}$ ... Viscosity

$\rho := 1.2$ ... Density of air (kg/m^3) $k := 0.024$ ... Conductivity (W/m.K)

$H_{fg} := 2500$ ... Latent heat of condensation (kJ/kg)

$p := 101325$ ... Standard atmospheric pressure (Pa)

Constants:

$$
\begin{pmatrix} c8 \\ c9 \\ c10 \\ c11 \\ c12 \\ c13 \\ c14 \\ c15 \\ c16 \\ c17 \\ c18 \end{pmatrix} := \begin{pmatrix} -5.8002206 \cdot 10^3 \\ 1.3914993 \\ -4.8640239 \cdot 10^{-2} \\ 4.1764768 \cdot 10^{-5} \\ -1.4452093 \cdot 10^{-8} \\ 6.5459673 \\ 6.54 \\ 14.526 \\ 0.7389 \\ 0.09486 \\ 0.4569 \end{pmatrix}
$$
   ... Constants in equations

93

$\Delta x := \dfrac{L}{N}$ ... Control volume length

$A_p := \pi \cdot D$ ... Control volume heat transfer area (m ^{2})

$m := V \cdot \rho \cdot \pi \cdot \left(\dfrac{D}{2}\right)^2 \cdot \Delta x$ ... Mass flow rate (kg/s) $m = 0.471$

Calculation of Nusselt number based on Dittus-Boelter relation for turbulent flow:

$Re := V \cdot \dfrac{D}{\nu}$ ... Reynolds number $Pr := 0.7$ ... Prandle number

$Nu := 0.023 \cdot Re^{0.8} \cdot Pr^{0.3}$ ... Dittus-Boelter correlation for turbulent flow in duct

$Re = 6.897 \times 10^4$ $Nu = 153.519$

$h_c := \left(Nu \cdot \dfrac{k}{D}\right)$ ... Convective heat transfer coefficient (W/ m ^{2}.K)

$h_c := if\left(h_c > 5, h_c, 5\right)$ $h_c = 7.369$

$h_m := \dfrac{h_c}{\rho \cdot c}$ ... Convective mass transfer coefficient (m/s) $h_m = 6.141 \times 10^{-3}$

$U := \dfrac{A_p \cdot h_c}{c \cdot m}$ $U = 0.025$

$a1 := \dfrac{\pi \cdot \left(\dfrac{D}{2}\right)^2 \cdot \dfrac{L}{N \cdot 10} \cdot c \cdot \rho \cdot V}{\pi \cdot D \cdot h_c \cdot \dfrac{L}{N \cdot 10}}$ $a1 = 40.712$

$$\begin{pmatrix} TT \\ w \\ RH \\ L \end{pmatrix} :=$$

$t \leftarrow t_o$ Initial condition

$RH \leftarrow RH_o$

$T_o \leftarrow 273.15 + t_o$

$P_{ws0} \leftarrow \exp\left(\dfrac{c8}{T_o} + c9 + c10 \cdot T_o + c11 \cdot T_o^2 + c12 \cdot T_o^3 + c13 \cdot \ln\left(T_o\right) \right)$

$p_{v0} \leftarrow RH_o \cdot p_{ws0}$

$w_o \leftarrow 0.62198 \cdot \dfrac{p_{v0}}{101325 - p_{v0}}$

$t_s \leftarrow t_{so}$

$T_s \leftarrow 273.15 + t_s$

$p_{wss} \leftarrow \exp\left(\dfrac{c8}{T_s} + c9 + c10 \cdot T_s + c11 \cdot T_s^2 + c12 \cdot T_s^3 + c13 \cdot \ln\left(T_s\right) \right)$

$p_{vs} \leftarrow 1 \cdot p_{wss}$

$w_s \leftarrow 0.62198 \cdot \dfrac{p_{vs}}{101325 - p_{vs}}$

for $i \in 1 .. 50$

    $T \leftarrow 273.15 + t$

    $p_{ws} \leftarrow \exp\left(\dfrac{c8}{T} + c9 + c10 \cdot T + c11 \cdot T^2 + c12 \cdot T^3 + c13 \cdot \ln(T) \right)$

    $p_w \leftarrow RH \cdot p_{ws}$

    $t_d \leftarrow c14 + c15 \cdot \ln\left(\dfrac{p_w}{1000}\right) + c16 \cdot \ln\left(\dfrac{p_w}{1000}\right)^2 + c17 \cdot \ln\left(\dfrac{p_w}{1000}\right)^3 + c18 \cdot \left(\dfrac{p_w}{1000}\right)^{0.1984}$

    $w \leftarrow 0.62198 \cdot \dfrac{p_w}{101325 - p_w}$ Dewpoint temp of each control volume.

    $\Delta t \leftarrow t_s - t_d$

    if $\Delta t > 0$ Case without condensation

        $w \leftarrow w$

        for $j \in 0 .. 9$

            $tt \leftarrow t$

$$tt \leftarrow t_s + \left(tt - t_s\right) \cdot e^{\dfrac{-j}{\dfrac{10 \cdot 50}{a1}}}$$

$$ttt_j \leftarrow tt$$

$$t_m \leftarrow \dfrac{\sum ttt}{10}$$ 　　　　　　Temperature at each element

$$t \leftarrow t - U \cdot \left(t_m - t_s\right)$$

$$T \leftarrow 273.15 + t$$

$$p_{ws} \leftarrow \exp\left(\dfrac{c8}{T} + c9 + c10 \cdot T + c11 \cdot T^2 + c12 \cdot T^3 + c13 \cdot \ln(T)\right)$$

$$p_w \leftarrow \dfrac{101325 \cdot w}{0.62198 + w}$$

$$RH \leftarrow \dfrac{p_w}{p_{ws}}$$ 　　　　　Temperature and RH at control volume

otherwise 　　　　　　　　　　　　　　Case with condensation

$$w_p \leftarrow w - \dfrac{h_m \cdot \rho \cdot A_p}{m} \cdot \left(w - w_s\right)$$

for $j \in 0..9$

$$tt \leftarrow t$$

$$tt \leftarrow t_s + \left(tt - t_s\right) \cdot e^{\dfrac{-j}{\dfrac{10 \cdot 50}{a1}}}$$ 　　　　Temperature at each element

$$ttt_j \leftarrow tt$$

$$t_m \leftarrow \dfrac{\sum ttt}{10}$$

$$t \leftarrow t + \dfrac{w_p - w}{c} \cdot H_{fg} - U \cdot \left(t_m - t_s\right)$$

$$w \leftarrow w_p$$

$$T \leftarrow 273.15 + t$$

$$p_{ws} \leftarrow \exp\left(\dfrac{c8}{T} + c9 + c10 \cdot T + c11 \cdot T^2 + c12 \cdot T^3 + c13 \cdot \ln(T)\right)$$

$$p_w \leftarrow \dfrac{101325 \cdot w}{0.62198 + w}$$

$$RH \leftarrow \dfrac{p_w}{p_{ws}}$$ 　　　　Temperature and RH at control volume

$$t_{out_0} \leftarrow t_o$$

$$t_{out_i} \leftarrow t$$

96

$t_{out_0} \leftarrow t_o$

$t_{out_i} \leftarrow t$

$w_{out_0} \leftarrow w_o$

$w_{out_i} \leftarrow w$

$RH_{out_0} \leftarrow RH_o$

$RH_{out_i} \leftarrow RH$

$td_i \leftarrow t_d$

$L_i \leftarrow i$

$\begin{pmatrix} t_{out} \\ w_{out} \\ RH_{out} \\ L \end{pmatrix}$

$TT =$

	0
0	30
1	29.607
2	29.223
3	28.848
4	28.483
5	28.127
6	27.78
7	27.441
8	27.11
9	26.788
10	26.473
11	26.167
12	25.867
13	25.576
14	25.291
15	25.013

$w =$

	0
0	0.019
1	0.019
2	0.018
3	0.018
4	0.018
5	0.018
6	0.018
7	0.017
8	0.017
9	0.017
10	0.017
11	0.017
12	0.017
13	0.016
14	0.016
15	0.016

$RH =$

	0
0	0.7
1	0.708
2	0.716
3	0.724
4	0.731
5	0.738
6	0.746
7	0.753
8	0.76
9	0.766
10	0.773
11	0.779
12	0.786
13	0.792
14	0.798
15	0.804

APPENDIX E:

CALCULATION OF FAN POWER AND SYSTEM COP

degC := 1

i := 1,2..10 X_i := i·5·m   length of tube   D := 0.5·m   diameter of tube

Hvi := 4·m   length of inlet vertical tube Hvo := 15·m length of outlet vertical tube

$V := 3 \frac{m}{s}$ $Q := \pi \cdot \frac{D^2}{4} \cdot V$ $Q = 2.121 \times 10^3 \frac{m^3}{hr}$

T_o := 26.5·degC   inlet air temperature T_a := 16·degC   outlet air temperature

$\rho := 1.2 \cdot \frac{kg}{m^3}$ density of air $c := 1000 \cdot \frac{joule}{kg \cdot degC}$ specific heat of air

ε := 3   roughness factor

Losses in inlet and vertical section

Cs := 5   pressure loss coefficient for Inlet screen and filter

Ct := 0.4   pressure loss coefficient for two 90 degree turn with turning vanes

Cf := 0.5   pressure loss coefficient in fan

Cs := 40   pressure loss coefficient in distributing pipes

$Re := 66400 \cdot D \cdot V \cdot \frac{s}{m^2}$ $f := 0.11 \cdot \left(\frac{\varepsilon \cdot m}{D \cdot 1000} + \frac{68}{Re} \right)^{0.25}$ f = 0.031

$\Delta Pvertical := f \cdot (Hvi + Hvo) \cdot \rho \cdot \frac{V^2}{2 \cdot D}$

Losses in inlet and vertical section

$\Delta Phoriz := f \cdot X_i \cdot \rho \cdot \frac{V^2}{2 \cdot D}$

Total losses:

$dPtotal := \left[\frac{\rho}{2} \cdot (Cs + Ct + Cf + Cs) \cdot V^2 \right] + \left(\Delta Pvertical + \Delta Phoriz \right)$

99

$Power_i := dPtotal_i \cdot Q$

	0
0	0
1	262.134
2	263.134
3	264.135
4	265.135
5	266.135
6	267.136
7	268.136
8	269.137
9	270.137
10	271.137

$Power = \quad$ W   power input (fan

$$m := V \cdot \rho \cdot \pi \cdot \left(\frac{D}{2}\right)^2 \qquad m = 2.545 \times 10^3 \frac{kg}{hr} \qquad \text{mass flow rate}$$

$$q := m \cdot c \cdot \left(T_o - T_a\right) \qquad q = 7.422 \times 10^3 \, W \qquad \text{thermal gains}$$

Distance along windtower (X)

$$COP := \frac{q}{Power_5} \qquad COP = 27.888$$